ACS OMEGA

Open Access

http://pubs.acs.org/journal/acsodf

Review

Natural Nano-Minerals (NNMs): Conception, Classification and Their Biomedical Composites

Feng Feng, Yihe Zhang,* Xiao Zhang, Bin Mu, Wenjie Qu, and Peixia Wang*

Cite This: *ACS Omega* 2024, 9, 17760−17783

Read Online

ACCESS | Metrics & More | Article Recommendations

ABSTRACT: Natural nano-minerals (NNMs) are minerals that are derived from nature with a size of less than 100 nm in at least one dimension in size. NNMs have a number of excellent properties due to their unique nanostructure and have been applied in various fields in recent years. They are rising stars in various disciplines, such as materials, biomedicine, and chemistry, taking advantage of their huge surface area, multiple active sites, excellent adsorption capacity, large quantity, low cost, and nontoxicity, etc. To provide a more comprehensive overview of NNMs and the biomedical applications of NNMs-based nanocomposites, this review classifies NNMs into three types by dimension, lists the structure and properties of typical NNMs, and illustrates their biomedical applications. Furthermore, a novel concept of natural nanomineral medical materials (NNMMs) is proposed, focusing on the medical value of NNMs. In addition, this review attempts to address the current challenges and delineate future directions for the advancement of NNMs. With the deepening of biomedical applications, it is believed that NNMMMs will inevitably play an important role in the field of human health and contribute to its promotion.

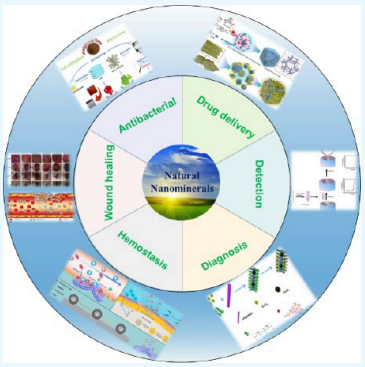

1. INTRODUCTION

Natural nano-minerals (NNMs) are derived from nature and have at least one dimension smaller than 100 nm in size,[1] which are mainly hydrous aluminum silicate minerals, such as montmorillonite (Mt), attapulgite (APT),[2] sepiolite, kaolinite (Kaol), etc. NNMs exhibit excellent physicochemical properties that benefit from the nanosize and unique structure, such as bulking, catalytic properties, plasticity and exchangeability of adsorbed ions.[3] The use of NNMs dates back to human civilization. Early on, NNMs were used to stop bleeding and to treat diarrhea. NNMs have also contributed to many works of art, such as the Mayan blue in the Mayan civilization and the Jingdezhen ceramics. In addition, NNMs are also found in buildings, mainly acting as matrix and binder before the age of concrete. With the development of characterization techniques, the structure of NNMs has been thoroughly analyzed, and their function has been further expanded. At present, NNMs and their derivatives are widely used in various fields such as geology, cosmetology, material science, pharmaceutical science, medicine, food science and biotechnology.[4−6] In addition, the unique properties such as environmental friendliness, good biocompatibility, abundant reserves, and ease of modification, etc. promote NNMs as a good alternative to biomedical materials.

Biomedical materials[7] are materials used in medicine, including sensing, detection, diagnosis, therapy, tissue repair, organ regeneration, in situ cell therapy,[8] vascularization in the organoid vascularization,[9] etc. Bone defect repair[10] has also received much attention in recent years. Especially in organoid research and sensing analysis, biomedical materials have become an important branch of modern materials science.[11,12] With the booming development of biotechnology[7] and the increasing improvement of health requirements, more and more biomedical materials such as graphene,[13,14] metal−organic frameworks (MOFs),[15] maximally exfoliated two-dimensional carbides and nitrides (MXenes)[16] and layered double hydroxide (LDH)[17] have been discovered and are receiving extensive attention from scientists.[18−22] Although, considerable progress has been made over the decades, some biomaterials present problems such as difficult preparation, high cost, poor biocompatibility and tolerability,[23−26] which limit further applications in the treatment of diseases such as cancer, cardiovascular diseases,[27−29] obesity, chronic diseases and, etc.[30] The environmental impact of medical waste is also a major concern. Large quantities of medical waste are produced each year, which endangers the environment and poses a serious threat to public health. It causes water pollution, poor air quality, and radioactive contamination.[31] For example, the amount of medical waste, including disposable masks, gowns, goggles, and gloves, has

Received: January 20, 2024
Revised: March 15, 2024
Accepted: March 25, 2024
Published: April 8, 2024

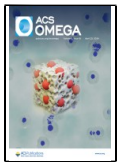

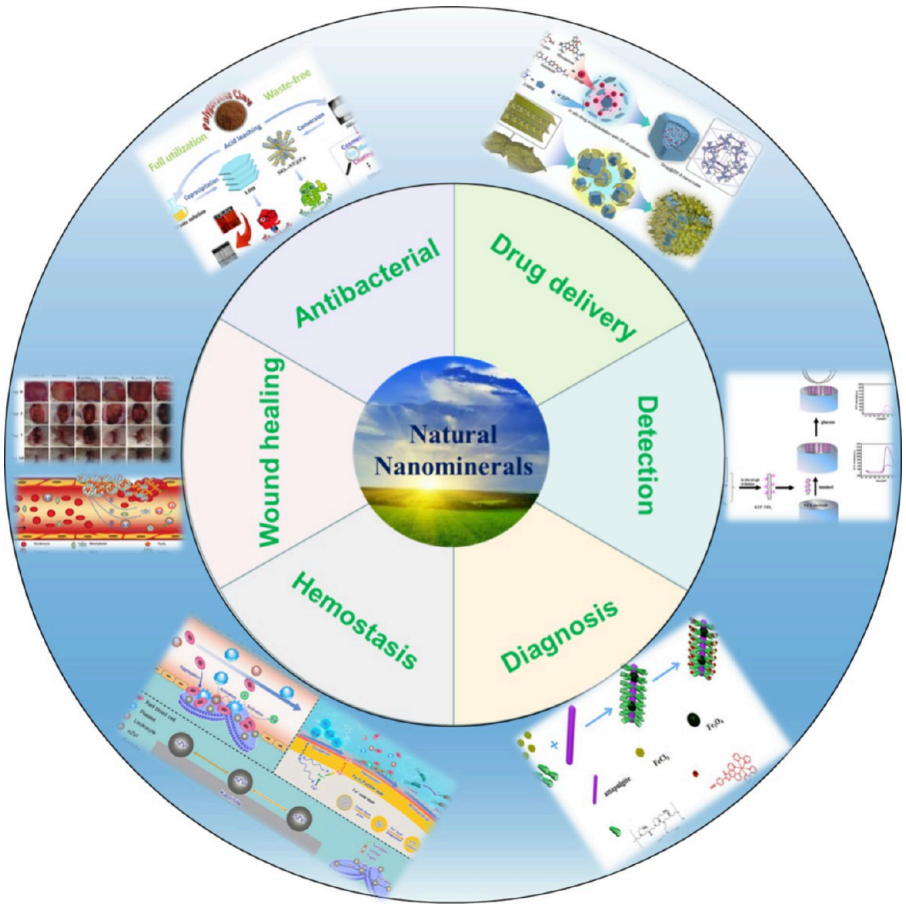

Figure 1. Biomedical applications of NNMs. Reprinted with permission from refs 43,46−50. Copyright 2023 Elsevier, 2020 Elsevier, 2020 American Chemical Society, 2016, Elsevier, 2017 Royal Society of Chemistry, 2018 Wiley.

increased significantly in recent years due to the emergence of pandemics[32,33] such as COVID-19.[34] This waste can also contribute to the spread of infectious diseases, such as AIDS, cholera, typhoid, and respiratory complications.

Therefore, novel biomaterials should be discovered and developed, taking into account their practical performance, economic viability and environmental impact. In contrast to some traditional and emerging biomaterials, NNMs are inherently natural, cost-effective, biocompatible, and environmentally friendly.[35,36] Benefiting from their unique structure and excellent physicochemical properties, NNMs are becoming a promising candidate for biomedical materials to overcome the shortcomings of various current biomedical materials. Compared to artificially prepared materials such as titanium alloys, hydrogels, polylactic acid, and zirconia, NNMs do not require preparation. Used as a biomaterials, they exhibit good biocompatibility due to their composition, which resembles the primary elements of the earth and their nontoxic nature.[37] Besides, the presence of numerous hydroxyl groups on their surface makes them easily modifiable by organic molecule, allowing for simple modifications for functional loading or to enhance biocompatibility.[38] In addition, are available in a range of dimensions depending on the size required.[39] Also, as biomaterials are used in large quantities, they are environmentally friendly and do not cause damage to nature on their own.[40,41]

As inorganic nonmetallic materials from nature, NNMs have a stable structure, large specific surface area, exchangeable ions, and special nanosized effects that are widely studied in antibacterial,[42] drug delivery, catalysis and hemostasis.[43] Besides, when NNMs are used as drug carriers, the dosage of existing drugs can be reduced through controlled release systems, thus favoring problems such as overdosing and environmental pollution. Belkadi et al.[44] synthesized inorganic−organic hybrid materials by incorporating amoxicillin (AMO) into the interlayer space of natural bentonite (N-BENT) from western Algeria, thereby reducing the adverse effects of AMO and the pollution caused by its disposal in the environment. NNMs are also used to adsorb pharmaceuticals from the environment. Kryuchkova et al.[45] investigated the adsorption properties of pristine Mt and stearyltrimethylammonium-modified Mt (Mt-STA) for drugs such as carbamazepine, ibuprofen and paracetamol. Mt-STA was shown to be a promising adsorbent for the removal of hydrophobic organic pollutants from wastewater. Furthermore, Mt-STA can be used not only for wastewater treatment but also for drug overdose detoxification due to its high drug capacity. Figure 1 shows NNMs that have been used in medicine in recent years.[43,46−51] As candidates for biomedical materials, NNMs are high-yield and low-cost, which is of great importance for the current huge demand for biomedical materials. Currently, NNMs are abundantly available[52] and are found in a wide range of rocks and soils.[53] In addition, NNMs are also being applied to recyclable use materials. For

https://doi.org/10.1021/acsomega.4c00674
ACS Omega 2024, 9, 17760−17783

example, M. Majka et al.[54] prepared nanocomposites of polypropylene and dry organic Mt (PP/OMt) by melt blending. The resulting pyrolyzed fillers can be used to create new composites. Therefore, NNMs are a sustainable alternative to medical materials due to their good storability and recyclability, which aligns with the concept of sustainable development.

NNMs are coming of age in biomedicine. This review provides a comprehensive overview of the latest research on NNMs in biomedical materials. First, NNMs are classified into three categories according to nanomorphology. Then, recent advances, applications and strengths are summarized aiming to provide an in-depth understanding of the relationship between the physicochemical properties and their performance. An outlook on their future directions and challenges is also given. Importantly, the concept of natural nanomineral medical materials (NNMMs) is proposed to facilitate the interface between materials and biomedical research.

2. NNMS: CONCEPTION, ORIGIN AND CLASSIFICATION

2.1. Basic Conception of NNMs. In order to conduct a systematic study of NNMs, we define their scope as primarily natural clay minerals. As exploitable natural resources, the definition of NNMs needs to be standardized. The concept should include the following basic characteristics:

(1) Source. NNMs are derived from nature and are not synthetic.
(2) Reserves. NNMs need to be accumulated in significant quantities to achieve a sufficient scale for long-term use.
(3) Size. NNMs must meet the requirement that at least one dimension is less than 100 nm and exhibit nanosized effects and properties that are valuable for applications.

2.2. Origin. Tracing the origin of NNMs is important for their definition and study. NNMs originated in the Earth's crust and have undergone long climatic, hydrological and geological processes,[55−58] including rock weathering, sedimentation and mineralization.[4,5] Specifically, NNMs in rocks have been fractured, dissolved and recrystallized to form layers and nanostructures, which have gradually been deposited and aggregated in groundwater and sedimentary environments.

2.3. Classification. Clear categorization is essential for the subsequent discussion and application of NNMs. A number of classifications are currently used to distinguish natural mineral materials. Scientists have divided minerals into two categories based on their state of crystallization, including crystalline and amorphous minerals. Crystalline minerals can be classified as 1:1 or 2:1 type, depending on their tetrahedral and octahedral structure. However, these classifications are based on structure and are not easily distinguished by morphology. To facilitate differentiation, we categorize them on the basis of nanodimensions for subsequent design and use. On this basis, NNMs can be classified into three different types, namely, zero-dimensional (0-D), one-dimensional (1-D) and two-dimensional (2-D).

2.3.1. 0-D NNMs. 0-D NNMs are the mineral minerals that typically have a nanospherical morphology. Examples include allophane, schwertmannite, and ferrihydrite.[4,5] For instance, allophane is a typical nanoclay that is amorphous in nature and has a hollow spherical shape (Figure 2(a)). Its theoretical

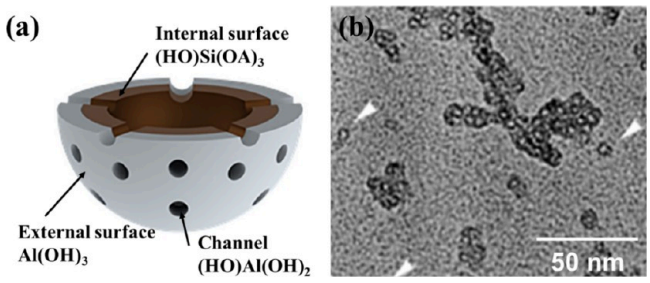

Figure 2. Structure and morphology of allophane. (a) Schematic representation of the structure of allophane, showing a hollow sphere with channels. Reprinted with permission from ref 59. Copyright 2021 Elsevier. (b) TEM image of allophane. Reprinted with permission from ref 60. Copyright 2017 Elsevier.

chemical composition is $(Al_2O_3)(SiO_2)_{1.3-2}\cdot 2.5-3H_2O$. Allophane has a diameter in the range of 3.5 to 5 nm and a shell-like wall, typically between 0.6 and 1.0 nm thick (Figure 2(b)). Another common 0-D NNMs is schwertmannite, with the chemical formula of $Fe_8O_8(OH)_{8-(2-3.5)}(SO_4)_{1-1.75}\cdot nH_2O$, which has spherical particles.

The natural spherical nanoenzymatic morphology of 0-D NNMs can be exploited as small molecule drug carriers or modifiers for functional materials.[61] In addition, their properties such as organic matter adsorption capacity, high porosity and specific surface area can be used to modulate microbial growth,[62] etc.

2.3.2. 1-D NNMs. Compared to 0-D NNMs, 1-D NNMs are more popular due to their special 1-D morphology. 1-D NNMs are those NNMs with a fibrous or needle-like structure, such as APT,[2] sepiolite, and imogolite, among others. Benefiting from the 1-D shape, they have a considerable specific surface area, which can reach hundreds of square meters per gram. In addition, NNMs have excellent absorbency and a large number of surface-active sites due to the differences in surface bonding, incomplete coordination of surface atoms, and electronic state within the rod crystal. For example, APT, also known as palygorskite, is a common type of 1-D NNMs with a rod-like structure (Figure 3(a)) and the ideal chemical formula of $Mg_5Si_8O_{20}(OH)_2(OH_2)_4\cdot 4H_2O$. Generally, they are found in nature as clustered crystal bundles (Figure 3(b)). Its crystal structure consists of 2:1 layered chains, with the tetrahedral wafer corners reversed at a certain distance in each layer of the unit structure layer, giving it a layered chain shape (Figure 3(c)).[63] Notably, APT reserves and production of APT are abundant worldwide. Currently, China, Brazil, and India are the main producers of APT, with a minimum annual global production of millions of tons per year, resulting in low costs.[64] Another typical 1-D NNM was halloysite nanotubes (HNTs), a type of silicate mineral, with an ideal molecular formula of $Al_2O_3\cdot 2SiO_2\cdot 4H_2O$ (Figure 3(f)). Unlike APT, the nanotubes of HNTs are dispersed, with an internal cavity of 10−15 nm, an external diameter of 20−150 nm, and a length of 50−1500 nm (Figure 3(d,e)). In recent years, the use of HNTs as a biocompatible carrier for loading has boomed due to their tubular shape. In addition, HNTs have a negative charge on the outer surface and a positive charge within the cavity at a pH range of 2−8. This allows HNTs to bind to drug

https://doi.org/10.1021/acsomega.4c00674
ACS Omega 2024, 9, 17760−17783

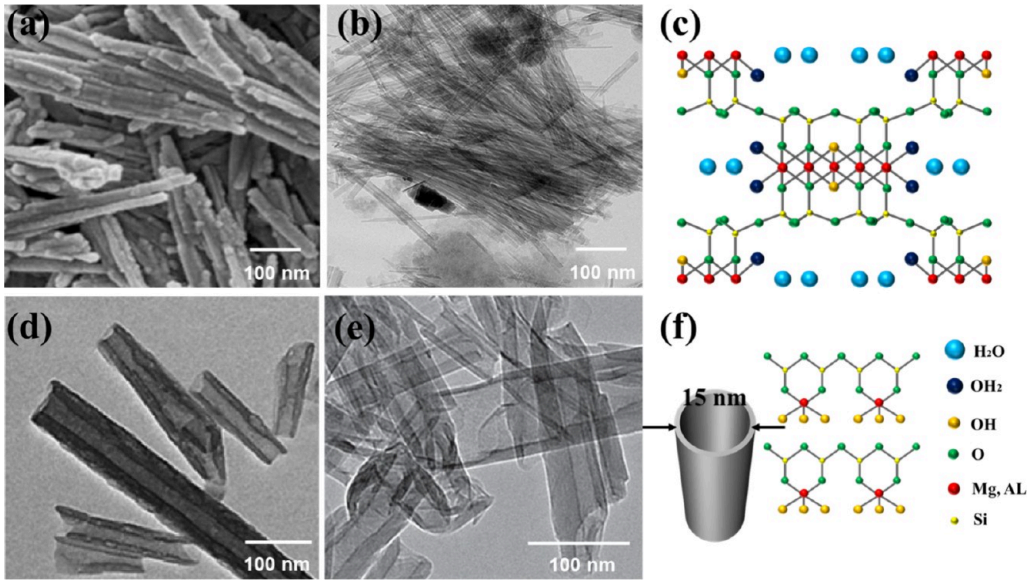

Figure 3. Morphologies and structures of APT and HNTs. (a) Scanning Electron Microscope (SEM). Reprinted with permission from ref 68. Copyright 2020 IOP Publishing Ltd. (b) Transmission Electron Microscope (TEM) of APT. Reprinted with permission from ref 64. Copyright 2019 Elsevier. (c) Crystalline structure of APT. (d) TEM image of HNTs. Reprinted with permission from ref 69. Copyright 2011 American Chemical Society. (e) High resolution TEM image of HNTs. Reprinted with permission from ref 70. Copyright 2018 The Royal Society. (f) Topography diagram and crystalline structure of HNTs.

molecules by manipulating the distribution or alteration of anions and cations on its surface, giving it potential capability as a controlled or sustained release agent. In addition, HNTs have been shown to be biocompatible. According to Fakhrullin et al.,[65−67] the nuclear morphology of cells did not change when exposed to primitive HNTs, demonstrating their high cytocompatibility.

In recent years, 1-D NNMs have been used in various fields due to their diversity and uniqueness. Currently, 1-D NNMs have attracted considerable research attention in the field of biomedicine due to their superior physicochemical properties, such as a negative surface potential, which facilitates the absorption of cationic molecules via electrostatic forces, and a large specific surface area, which provides numerous attachment points.[71,72] As a result, they have become popular drug delivery vehicles.

2.3.3. 2-D NNMs. In short, except for 0-D and 1-D NNMs, the rest are 2-D NNMs. The basic element of 2-D NNMs has a layered structure, including Mt, Kaol, hydrotalcite, and others. The layers are typically held together by chemical bonds within them and by van der Waals forces between them, and can be separated from each other by stacking. Specifically, Mt is a layered mineral consisting of hydrated aluminosilicate, with a theoretical chemical formula of $(Na, Ca)_{0.33}(Al, Mg)_2[Si_4O_{10}](OH)_2{\cdot}nH_2O$. Mt has a three-layer sheet structure (2:1 type) consisting of aluminum oxide octahedrons in the center and silicon oxide tetrahedra on the top and bottom. Apparently, the layered structure of Mt can be observed clearly under an SEM (Figure 4(a, b)), accompanied by monolayer thicknesses of less than 100 nm (Figure 4(c)). Notably, Mt has excellent ion exchange and intercalation properties due to its distinct layered structure. Another typical 2-NNMs is Kaol, which also consists of layers of silicon−oxygen tetrahedral sheets and "alternate" octahedral sheets. These layers are stacked along the *c*-axis to form a structural unit. And, the ideal formula for the Kaol layer is $Al_2SiO_5(OH)_4$, consisting of 46.54% SiO_2, 39.5% Al_2O_3, and

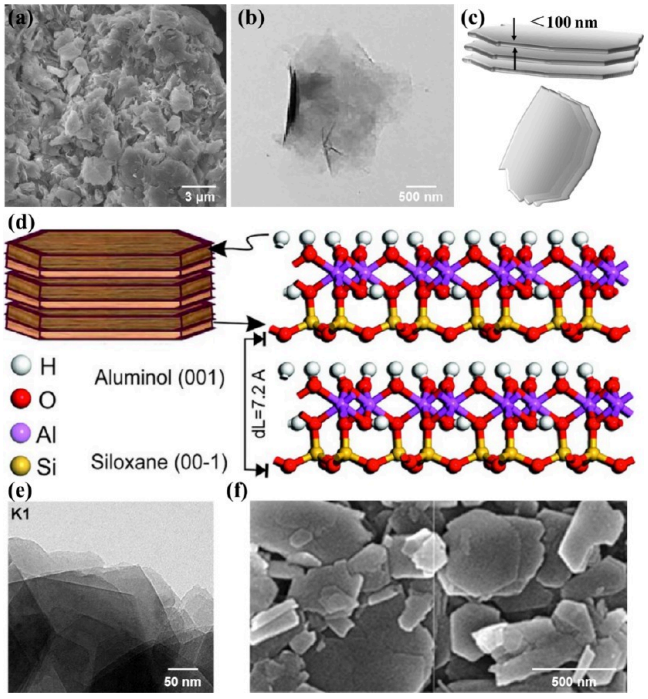

Figure 4. Morphology and structure of Mt and Kaol. (a) SEM of Mt. Reprinted with permission from ref 73. Copyright 2013 Springer. (b) TEM image of Mt. Reprinted with permission from ref 74. Copyright 2013 Elsevier. (c) Topography diagram of Mt. (d) Molecular simulation model of Kaol structure (1 × 2 × 2 unit cells) showing siloxane and aluminol surfaces. Reprinted with permission from ref 75. Copyright 2017 Elsevier. (e) TEM image of Kaol. K1 consisted mainly of large, irregularly arranged fragments with a natural close packing. Reprinted with permission from ref 76. Copyright 2019 Elsevier. (f) High-resolution TEM image of a kaol. Reprinted with permission from ref 77. Copyright 2022 Elsevier.

https://doi.org/10.1021/acsomega.4c00674
ACS Omega 2024, 9, 17760−17783

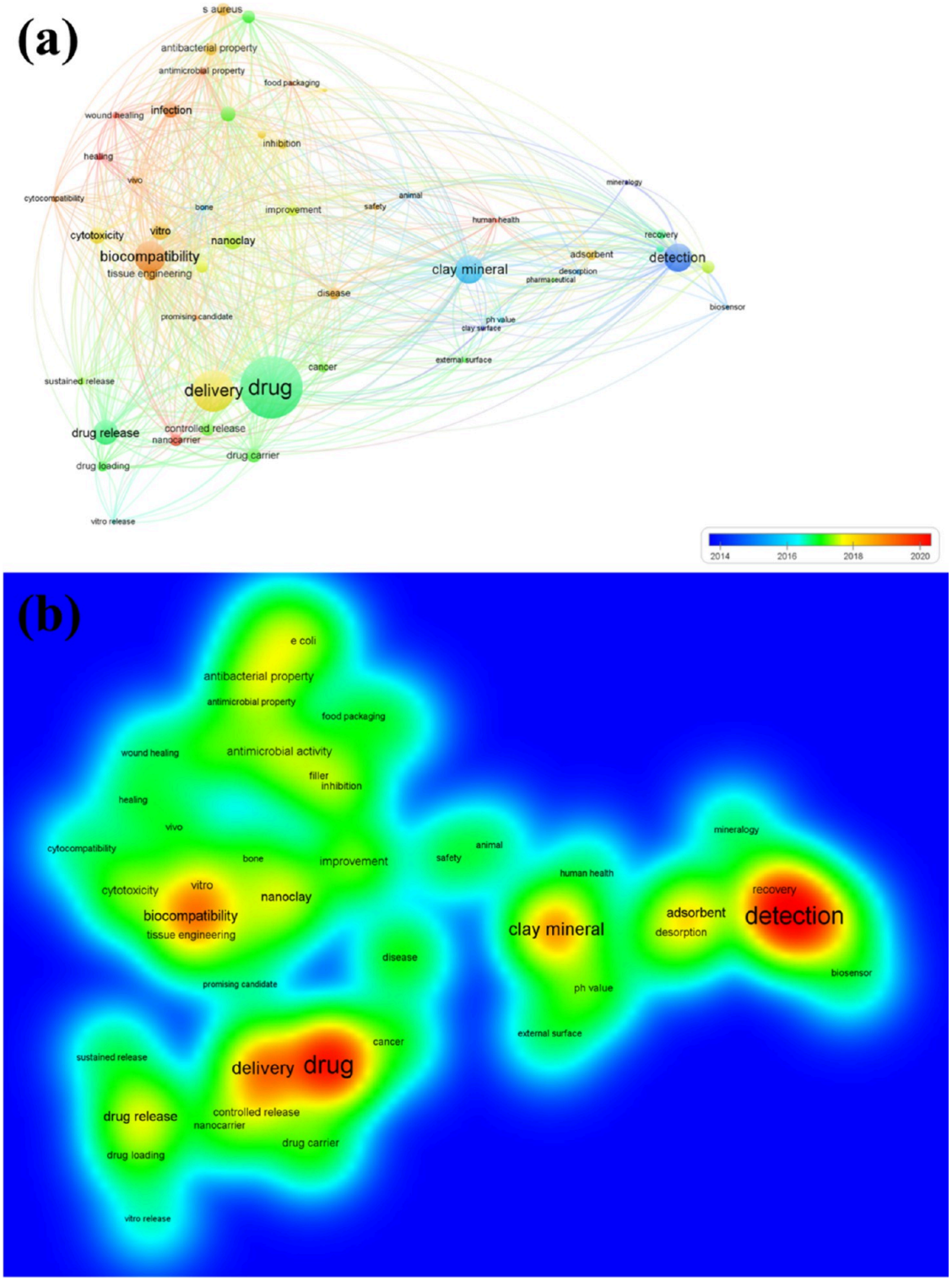

Figure 5. Overview of biomedical applications of NNMs. (a) Network visualization and (b) density visualization based on the reference for biomedical application and nanomineral keywords.

13.96% hydroxyl (Figure 4(d)). Most Kaol samples are dispersed powders with a cryptocrystalline structure, characterized by loose and massive aggregates. The characteristic hexagonal shape of Kaol is formed by stacked pseudohexagonal platelets, which dissociate seamlessly. In terms of morphology, the crystals of Kaol may have a self-shaped hexagonal plate, semihexagonal or other shaped flake, with a scale size generally ranging between 0.2 and 5 μm and a thickness of less than 200 nm (Figure 4(e, f)).

Nowadays, the interest in 2-D NNMs has increased due to their expandable planes and interacting properties. They are often used as a drug carrier due to its easily modifiable surface, which can be loaded with small molecules because of its large interlayer space and the presence of numerous hydrogen bonds on the surface.[78] Furthermore, its surface

https://doi.org/10.1021/acsomega.4c00674
ACS Omega 2024, 9, 17760−17783

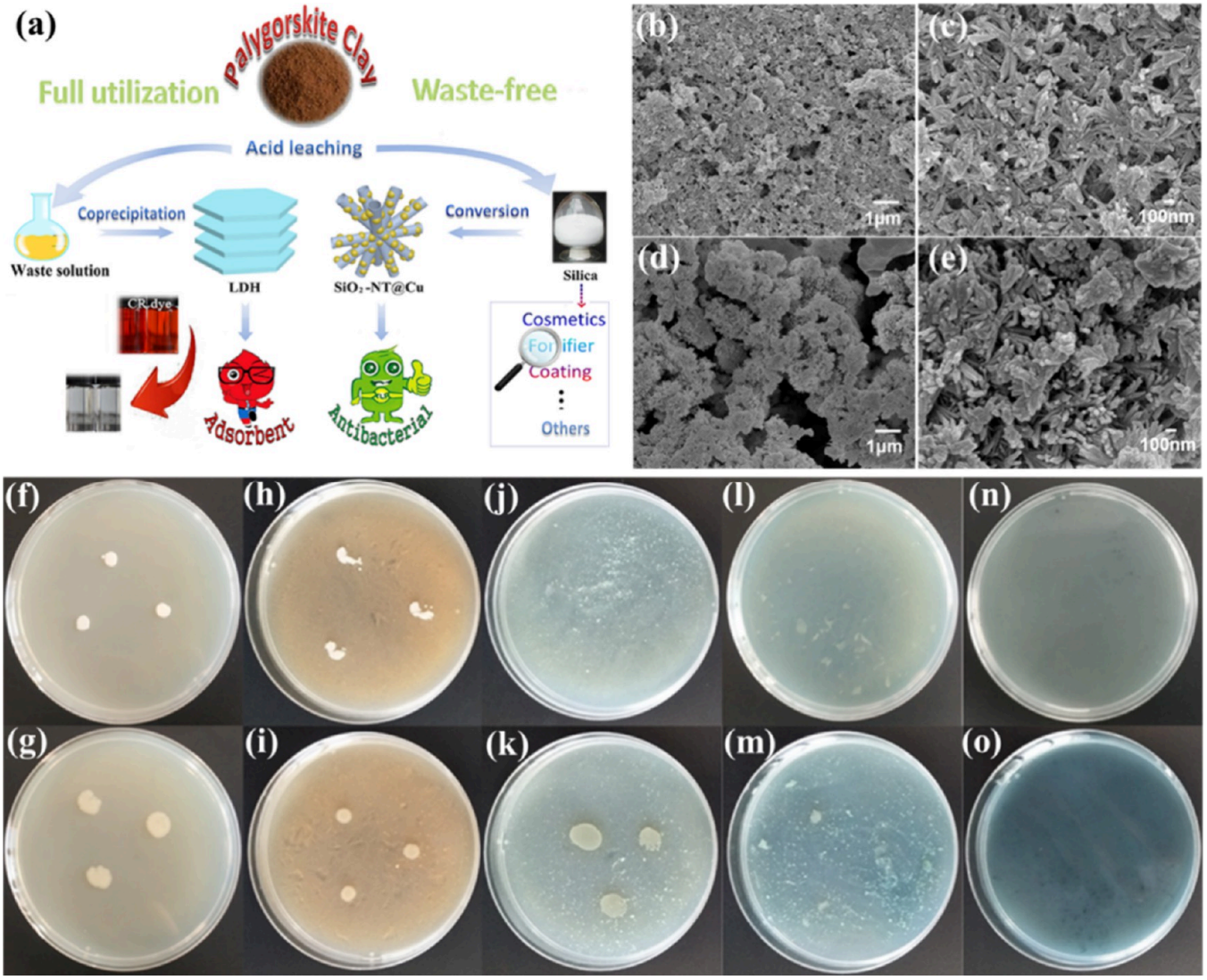

Figure 6. Overview of the antibacterial process using APT as a precursor. (a) Schematic diagram of the research for the utilization of raw APT to antibacterial. SEM images of (b, c) L-SiO_2−NT@Cu and (d, e) V-SiO_2−NT@Cu. The positive control of *S. aureus* (f) and *E. coli* (g). The digital photos of the bacteriostatic effects of crude APT for (h) *S. aureus* (2.0 mg/mL) and (i) *E. coli* (2.0 mg/mL), of $CuSiO_3$ for (j) *S. aureus* (2.0 mg/mL) and (k) *E. coli* (2.0 mg/mL), of L-SiO_2−NT@Cu for (l) *S. aureus* (1.0 mg/mL) and (m) *E. coli* (2.0 mg/mL), and of V-SiO_2−NT@Cu for (n) *S. aureus* (0.6 mg/mL) and (o) *E. coli* (2.0 mg/mL). Reprinted with permission from ref 46. Copyright 2019 Elsevier.

properties vary with pH, allowing it to act as a controlled or slow release for drug molecules.[79] In the latest field of nanozymes, they can also modify the cationic occupancy of ferrite, thus enhancing the enzyme-like activity of the composites.[80] Additionally, their good mechanical properties make them suitable additives for some hydrogels.[81] Their unique 2-D structure and good biocompatibility have made them a promising material in the fields of detection, diagnosis, and therapy.[82] Besides, 2-D NNMs have excellent intrinsic adsorption capacity and the ability to promote wound healing, allowing them to be used as wound dressings.

3. BIOMEDICAL APPLICATIONS OF COMPOSITES BASED ON NNMS

Due to their excellent biocompatibility, large specific surface area, high storage capacity, and low cost, NNMs and their derivatives have recently become increasingly popular among biomedical materials.[3] We reviewed and analyzed the most cited literature (Figure 5(a, b)). Since 2014, there have been several reports on the use of NNMs for detection. The preparation of nanocomposites using NNMs as sensors is a practical approach to achieve efficient detection. While the use of NNMs as nanocarriers for sustained, slow, or controlled release gained widespread attention starting from 2016, they were later developed, after 2018, for bone tissue engineering, antibacterial and anti-inflammatory materials, and wound healing due to their exceptional biocompatibility. Overall, the early development of NNMs focused on in vitro detection and drug delivery. Once their excellent biocompatibility had been demonstrated, the corresponding in vivo studies were carried out.

3.1. Antibacterial Materials. The development of biocompatible antibacterial materials that are efficient and effective is critical to reducing the risk of bacterial infections. Inorganic antibacterial materials are composed of supports infused with ions, oxides or photocatalytic materials (e.g., ZrO_2, TiO_2) and transition metals such as Ag, Cu, Zn, etc. that possess antibacterial properties. Many of these materials

https://doi.org/10.1021/acsomega.4c00674
ACS Omega 2024, 9, 17760−17783

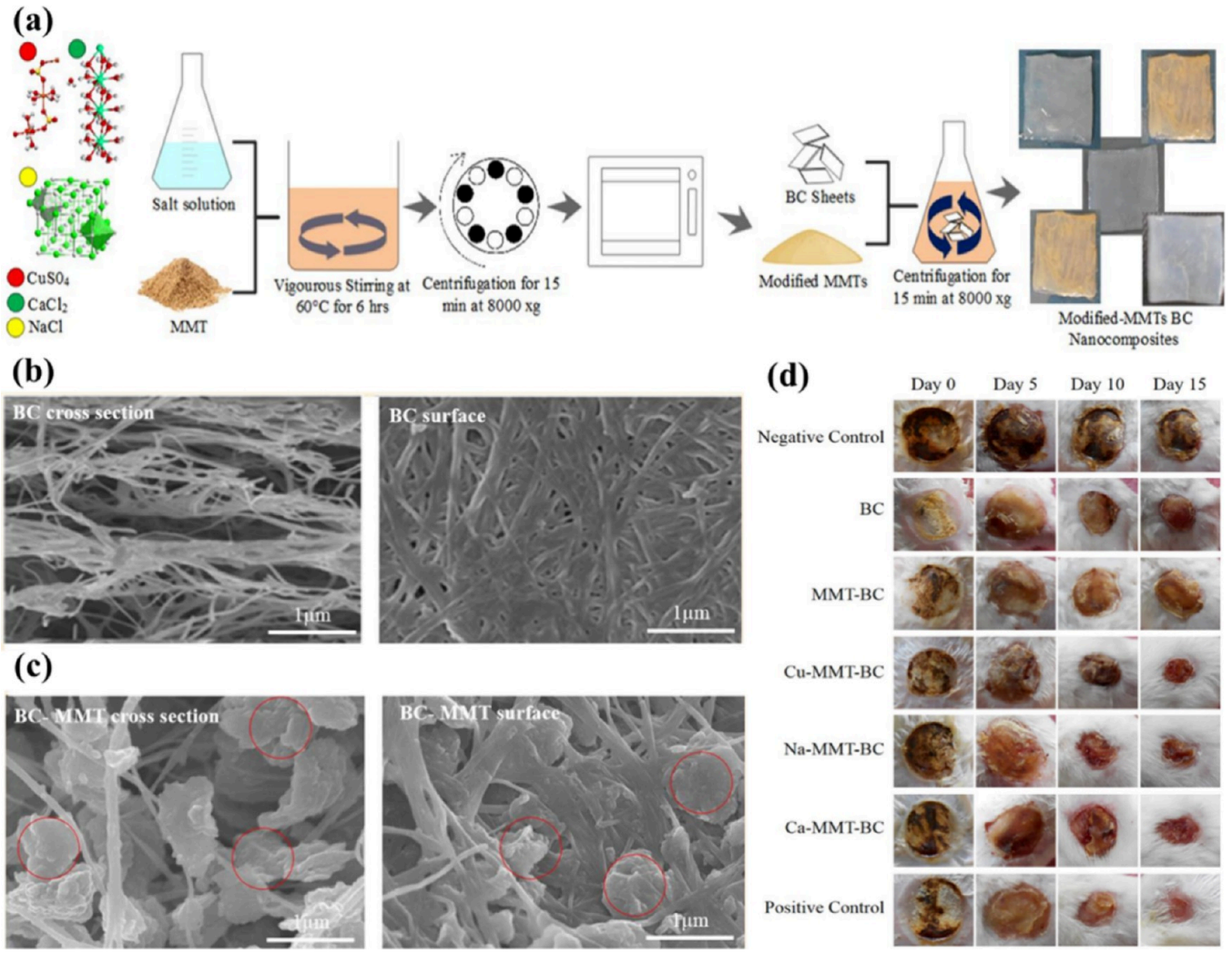

Figure 7. Mt-BC for antibacterial. (a) Schematic diagram illustrating the synthesis of a nanocomposite by modified Mt and BC nanocomposites. SEM images of (b) BC and (c) Mt-BC nanocomposites. (d) Representative photographs of wounds treated with Cu-Mt-BC, Na-Mt-BC, and Ca-Mt-BC, together with those of the negative control, BC, Mt-BC, and positive control groups were taken at different stages of the treatment process. Reprinted with permission from ref 85. Copyright 2018 Elsevier.

are nanomaterials with increased specific surface areas, allowing greater exposure of active sites. NNMs contain antibacterial atoms such as Fe and Cu due to their homogeneous substitution in the environment.[83] In addition, their nanomorphology results in a significant specific surface area, making them effective agents against bacteria both independently and as carriers.

To reduce reliance on antibiotics, Yang et al.[84] investigated the effect of Cu-modified APT (CM-APT) on the prevention and treatment of *Salmonella diarrhea* in vivo. According to in vitro antibacterial tests, CM-APT proved to be a viable substitute for conventional antibiotics in the treatment and prevention of animal diarrhea caused by *Salmonella*. Wang et al.[46] used APT as a precursor to obtain silica nanorods and metal ions to prepare a medical antibacterial composite (Figure 6(a)). Using the decomposed APT, they synthesized the SiO_2−NT@Cu nanocomposite in tubular form by two methods. First, they immersed the $CuSiO_3$ nanotube in a 5 mol/L aqueous solution of $NaBH_4$ under magnetic stirring. Then, the resulting mixture was heated to 70 °C to reduce Cu^{2+} into CuNPs according to the reaction given in equation (eq) (1) (the product was named L-SiO_2−NT@Cu). $CuSiO_3$ nanotubes were treated with H_2 flow at 450 °C for 3 h to reduce Cu^{2+} into CuNPs according to the reaction shown in eq 2 (the resulting product was named V-SiO_2−NT@Cu). After undergoing physical and chemical treatment, the APT retained its rod-like structure as shown in Figure 6(b-e). Furthermore, the antibacterial experiment showed that the SiO_2−NT@Cu nanocomposite was highly effective in inhibiting the growth of *E. coli* and *S. aureus*, with minimal inhibitory concentrations (MICs) of 2.0 and 0.6 mg/mL, respectively, as shown in Figure 6(f-o).

$$BH_4^- + 2Cu^{2+} + 3OH^- \rightarrow 2CuNPs + H_3BO_3 + 2H_2\uparrow \quad (1)$$

$$CuSiO_3 + H_2 \rightarrow CuNPs + SiO_2 + H_2O \quad (2)$$

Bacterial cellulose (BC) is a biopolymer known for its ability to heal wounds and regenerate tissue. However, BC's inability to repel bacteria limits its use in biomedicine. The research of Wahid et al.'s research[85] proposed to create new artificial burn substitutes by combining the wound healing properties of BC with the antibacterial performance of modified Mt (Figure 7(a)). SEM images (Figure 7(b, c))

https://doi.org/10.1021/acsomega.4c00674
ACS Omega 2024, 9, 17760−17783

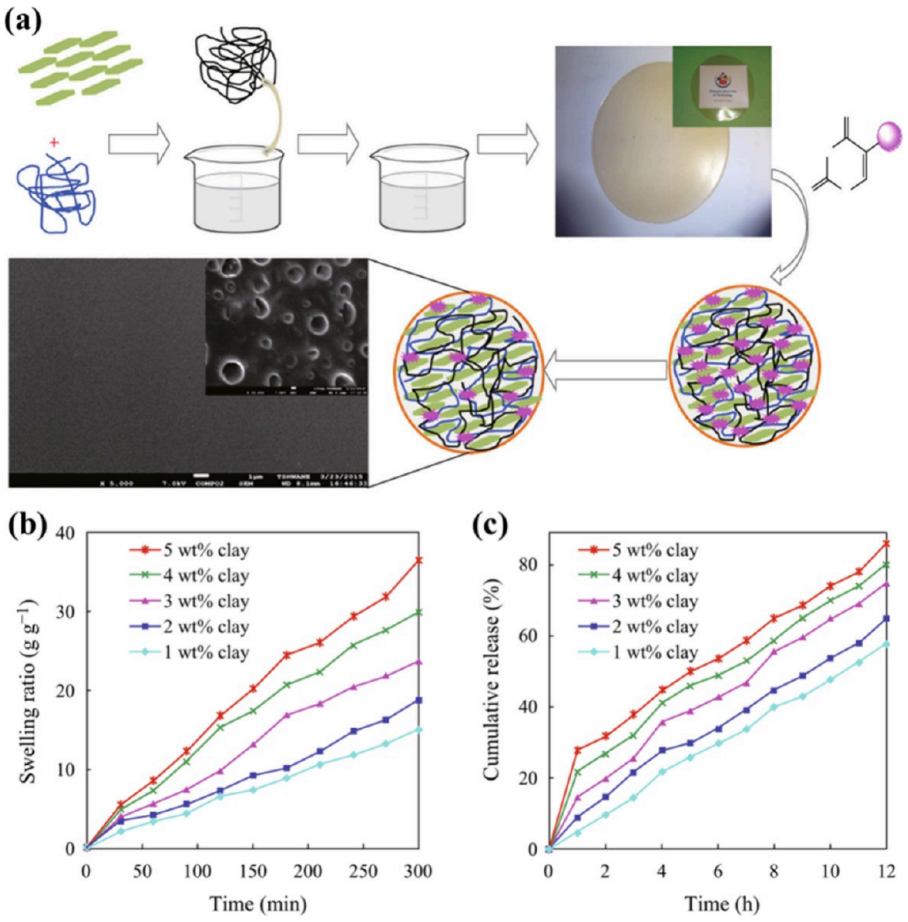

Figure 8. Preparation, swelling capacity and 5-FU release properties of chitosan/PVA/Na+-Mt. Chitosan/PVA/Na+-Mt (a) Schematic diagram of the preparation process of chitosan/PVA/Na+-Mt loaded with 5-FU. (b) Swelling capacity and (c) 5-FU release of chitosan/PVA/Na+-Mt with different Na+-Mt contents. Reprinted with permission from ref 86. Copyright 2016 Springer.

confirmed the presence of Mt on the surface and substrate. The modified Mt-BC nanocomposite showed a clear zone of inhibition in the test. The animal experiment proved that the mouse treated with Mt-BC nanocomposite showed improved wound healing activity through tissue regeneration, healthy granulation, re-epithelialization, and vascularization (Figure 7(d)). These results suggested that the modified Mt-BC nanocomposite can be used as a novel substitute for artificial skin and as a scaffold for tissue engineering in burn patients.

In addition to its intrinsic antimicrobial properties, Mt can also act as a reservoir for antimicrobial drugs, allowing for controlled or gradual release. Reddy et al.[86] carried out in vitro drug delivery studies by preparing a chitosan/PVA/Na+-Mt composite membrane loaded with 5-fluorouracil (5-FU) (Figure 8(a)), which exhibited significant inhibitory activity against both *Salmonella* (Gram-negative) and *S. aureus* (Gram-positive). Meanwhile, the rate of drug release could be regulated by modifying the amount of Mt (Figure 8(b, c)).

Ag is a frequently used inorganic antimicrobial agent. However, its high cost and poor biocompatibility restrict its use. Zhou et al.[87] developed simple and environmentally friendly(a rapid, straightforward, and eco-friendly) technique to prepare lecithin (LEC) modified silver(Ag)-based Mt (AgNPs@LEC-Mt) using silver nitrate. Figure 9(a) shows that the obtained AgNPs@LEC-Mt was biocompatible with L929 cells, provided that the concentration was below 25 μg/mL. In addition, the inhibition zone test suggested that the AgNPs@LEC-Mt had effective antibacterial activity against Gram-positive and Gram-negative bacteria (Figure 9(b)). And, the antibacterial property would be enhanced with increasing Ag concentration. Moreover, optical and SEM images showed significant antibacterial effect against *E. coli* and *S. aureus*, and bacterial morphology after treatment with AgNPs (0.8 M)@LEC-Mt compared to pure Mt (Figure 9(c-j)), indicating the importance of introducing antimicrobial metals. In addition, the introduction of Mt effectively improved the biological toxicity of the composites. Essential oil (EO) is a natural organic antibacterial material. Souza et al.[88] evaluated the synergistic effect of carvacrol EO and Mt (called hybrid compound) incorporated in thermoplastic starch (TPS) films at different levels. The hybrid films showed antimicrobial activity against *E. coli* due to the synergistic effect of Mt and EO. The hybrid resulted in combined antimicrobial effects, probably due to the destabilization and partial destruction of the bacterial cell membrane, altering the permeability, respiration and electron transport of the *E. coli*. These research results can provide references for the future development of Mt-based membranes.

Kaol has been extensively researched and used in the development of antimicrobial composite materials in recent years. Yang et al.[89] prepared Fe_2O_3-Kaol, which showed potent antibacterial activity against *E. coli*. The synergy

https://doi.org/10.1021/acsomega.4c00674
ACS Omega 2024, 9, 17760−17783

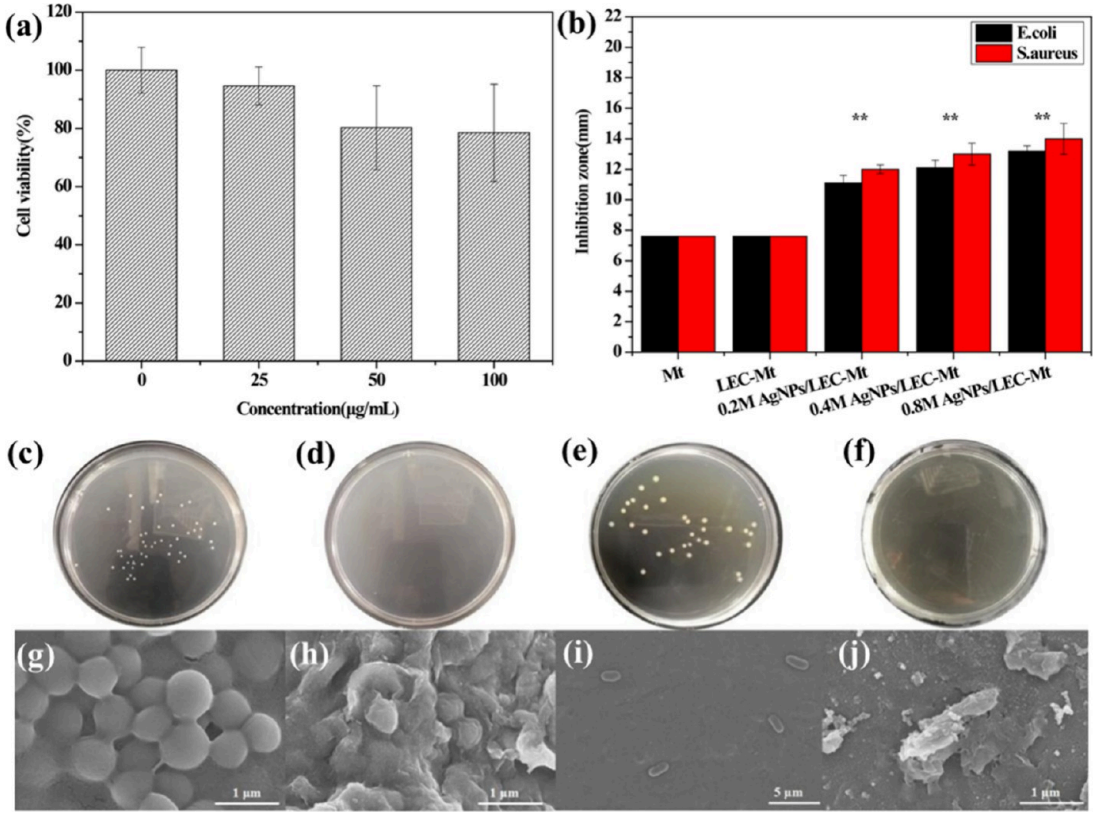

Figure 9. AgNPs@LEC-Mt for antibacterial application. (a) Cytotoxicity of AgNPs@LEC-Mt on cells L929. (b) Inhibition zone of AgNPs@LEC-Mt of different Ag content against strains *E. coli* and *S.aureus*. Optical images of antibacterial activities against *E. coli* by (c) Mt and (d) AgNPs(0.8 M)@LEC-Mt, and against *S.aureus* by (e) Mt and (f) AgNPs(0.8 M)@LEC- Mt. SEM images of bacterial of *S. aureus* (g) before and (h) after, and (i) *E. coli* before and (j) after treatment with AgNPs(0.8 M)@LEC- Mt. Reprinted with permission from ref 87. Copyright 2019 Elsevier.

provided by the well-dispersed Fe_2O_3 nanoparticles through the large specific surface area of Kaol was responsible for this activity (Figure 10(a)). The density of the Fe_2O_3 nanoparticle distribution significantly influenced the antibacterial activity, with optimal nanoparticle distribution yielding the highest antibacterial activity. Tripathy et al.[90] used the coprecipitation technique to prepare zinc (Zn) oxide/potassium and impregnated it in Kaol to synthesize an antibacterial composite substance (Figure 10(b)). Antibacterial experiments showed that the bacterial morphology progressively disintegrated under visible light treatment (PCD) progressively disintegrated over time (Figure 10(c-h)), probably due to oxidative stress caused by excessive amounts of superoxide radicals.

In addition to combining with inorganic antimicrobials, the antibacterial effect of Kaol can be enhanced by a good combination with organic antimicrobial agents. A Kaol-based organic antibacterial material (CA/Kaol) modified with chlorhexidine acetate (CA) was prepared by a dry process by Zhang et al.[91] The results showed that a synergistic promotion system between CA and kaol had been established. Kaol optimized and controlled the thermal stability of CA to achieve an on-demand burst/slow release mode. CA was mainly bound to the surface of Kaol by hydrogen bonding. This gave it antibacterial properties and improved organic compatibility.

In addition to their antibacterial properties, NNMs have been used in anti-inflammatory treatments. Wele et al.[92] investigated the anti-inflammatory activity of the croton oil-induced edema treatment and found that APT had anti-inflammatory properties. As such, APT may be useful in the treatment of conditions such as rheumatism, neurosis, and skin disorders.

The antibacterial application of NNMs is based on the following intrinsic properties: (1) NNMs have elements on their surface that fight disease-causing bacteria, such as Fe, Cu, etc. Some of these antimicrobial elements are immobilized on their surfaces, while others can be dissolved in a solution to contact the bacterial surface and sterilize it. (2) Some of the NNMs are due to the fact that NNMs have easily modifiable groups on their surface, which allows them to be loaded with compounds with antimicrobial factors. The advantage of minerals as antimicrobial agents is their good biocompatibility and ease of modification. In addition, their low cost is an advantage as an antimicrobial material that is in high demand.

3.2. Drug Delivery. The advent of functional nanomedicines has treated some of the most intractable diseases.[93] They have enabled drug molecules to enter the human body as ultrasmall trucks, and targeted drugs deliver drugs directly to the diseased area, reducing drug damage to normal human cells.[94] In addition, nanodelivery of drugs to improve their utilization or to achieve slow or controlled release is important for disease treatment and cost control. Although these functionalized drugs have made some progress in treating intractable diseases, they are still limited in terms of therapeutic efficacy and cost.[95] In general, nanodrug carriers usually need to have appropriate electrical properties,

https://doi.org/10.1021/acsomega.4c00674
ACS Omega 2024, 9, 17760−17783

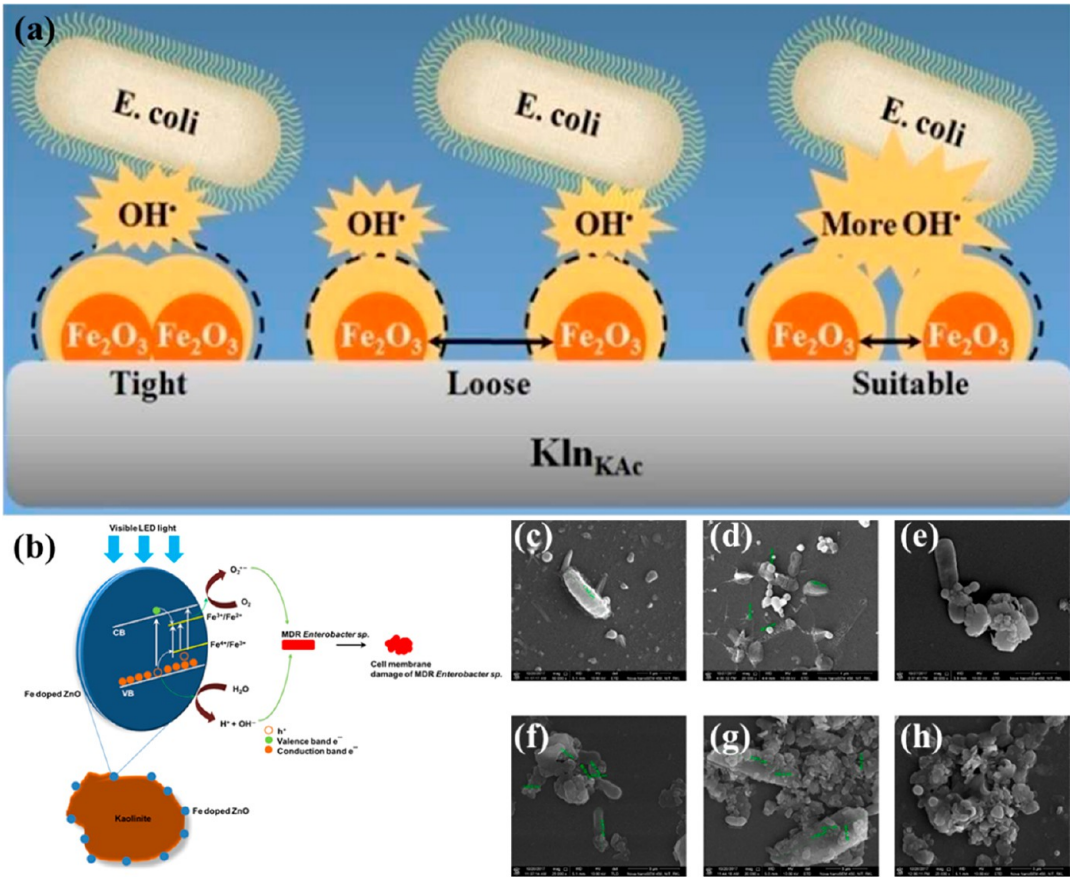

Figure 10. Antibacterial properties of Fe_2O_3−Kaol. (a) Schematic illustration of the antibacterial activity of Fe_2O_3−Kaol composites. Reprinted with permission from ref 89. Copyright 2017 Royal Society of Chemistry. (b) Schematic representation of the PCD of *Enterobacter sp.* using ZnO/Kaol under visible light.[90] (c), (d), and (e) show the Field Emission (FE) SEM images of untreated bacteria, photolysis-treated and dark control (with ZnO/Kaol loading = 150 mg/L) of MDR *Enterobacter sp.* at 120 min, respectively.[90] (f), (g) and (h) showed the FESEM microscopic images of MDR *Enterobacter sp.* subjected to visible light assisted PCD in the presence of ZnO/Kaol (with ZnO/Kaol loading = 150 mg/L) for 60-, 90-, and 120 min treatment, respectively.[90] Reprinted with permission from ref 90. Copyright 2018 Elsevier.

multiple loading sites, large surface or internal space and good biocompatibility. In addition to possess the above characteristics, the electrical, chemical binding and surface properties of NNMs change with pH or other treatments, making them a promising choice as nanodrug carriers. Besides, NNMs have the properties of large reserves and easy accessibility compared to artificially prepared ones. As a result, NNMs have made a splash in drug delivery in recent years.

The hollow tube and modifiable surface of HNTs have attracted interest in drug delivery for decades. The use of HNTs as carriers for drug delivery, sustained, and controlled release of drugs has been extensively reported. Zhang et al.[96] prepared a novel HNTs-based hydrogel with a "turn-on" fluorescence character upon H_2O_2 and used it to construct the H_2O_2-responsive drug delivery system, in which a coprecipitation method was proposed to obtain the drug-loaded HNTs (DHNTs) (Figure 11(a)). The experimental results showed that the morphology of the HNTs did not change before and after loading (Figure 11(b-e)). Other characterizations also showed that the drug was mainly loaded into the cavity and not attached to the outer surface of the HNTs. In the presence of H_2O_2, the boron−carbon bonds in the prepared hydrogel were broken, leading to degradation and a responsive release (Figure 11(f, g)). At physiological concentrations ($[H_2O_2]$ = 0.02 μM) hardly any drug release occurs, whereas at pathological concentrations ($[H_2O_2]$ = 200 μM), complete release (>90%) can be achieved (Figure 11(h)). The release kinetic curve illustrates the stability of the kinetics (Figure 11(i)).

Controlled release can also be achieved by modifying the surface of HNTs. Lvov et al.[97] used octadecylphosphonic acid to selectively modify the lumen of HNTs (Figure 12(a)). Adsorption studies had shown that the hydrophobized HNTs adsorbed more ferrocene than its hydrophilic derivative (ferrocene carboxylic acid), and the equilibrium absorption isotherm of ferrocene was linear, indicating that these molecules are driven into the lumen by separation from the polar solvent. The results showed that the complex can absorb hydrophobic molecules as a physically adsorbed sponge (Figure 12(b,c)). This research has showed that the different chemical properties of the inner and outer surfaces of HNTs can be used for selective modification, so as to realize various applications from water purification to drug immobilization and controlled release.[97] In addition to 1-D HNTs, APT are also used as drug loading and release. Viseras et al.[98] successfully prepared cross-linked APT/chitosan composites using tripolyphosphate as the cross-linking agent. The addition of a certain amount of APT not only improved the embedding effect of the composite microspheres, but also influenced the drug release and prolonged the release time of diclofenac. Therefore, the

https://doi.org/10.1021/acsomega.4c00674
ACS Omega 2024, 9, 17760−17783

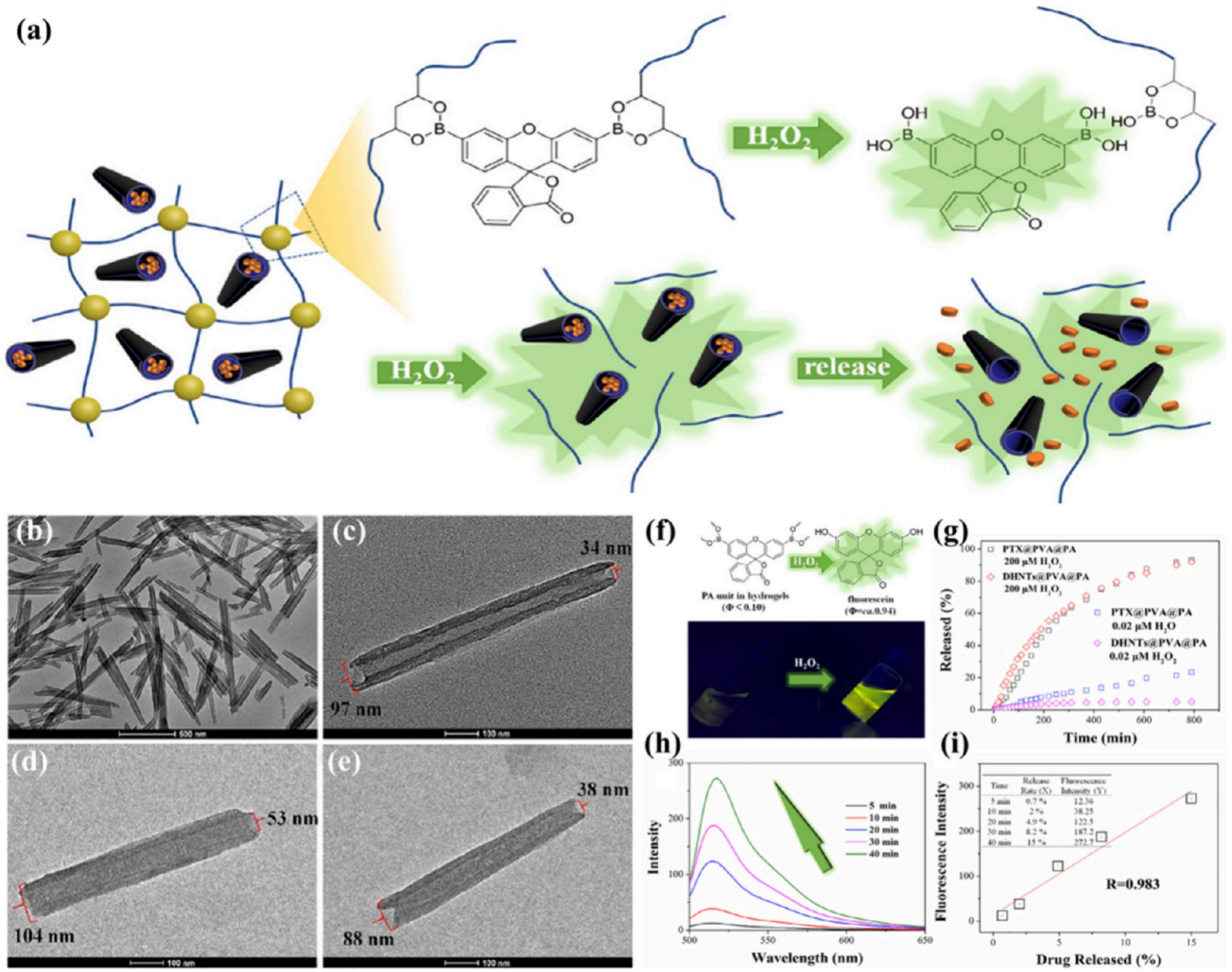

Figure 11. Drug release properties of HNTs-based composites. (a) H_2O_2-sensitive release mechanism of DHNTs@PVA@PA. TEM images of (b, c) HNTs and (d, e) DHNTs. (f) The transformation mechanism of arylboronates to phenols to give fluorescein with high fluorescence in the presence of H_2O_2. (g) The changes of DHNTs@PVA@PA from nonfluorescent to fluorescent. (h) The drug release profiles in different concertation of H_2O_2. (h) The fluorescence spectra of the release medium (H_2O_2 = 200 μM) after the addition of DHNTs@PVA@PA. (i) Plots of fluorescence intensity versus the drug release rate. Reprinted with permission from ref 96. Copyright 2020 Elsevier.

incorporation of APT into biopolymers can be used for the sustained release of drugs and other biologically active particles.

The planar and interlayer space of a 2-D NNMs is also an ideal property for drug delivery. For example, Mt, is widely used for drug delivery due to its large interlayer space and good adsorption properties. Oral administration faces the physiological limitations of the gastrointestinal tract (GIT) and causes irritation of the gastrointestinal mucosa. Inspired by the mucosal nutritive function of zinc (Zn) and Mt, Bai et al.[47] developed a Mt-coated zeolitic imidazolate framework (M-ZIF-8) capable of encapsulating and releasing drugs (Figure 13(a)). The ZIF-8 encapsulated drug can maintain its internal structure, and the Mt layer enhances adhesion and optimizes drug release. Meanwhile, it had good biocompatibility with SGC7901 and CT26 cells (Figure 13(b)). M-ZIF-8 not only achieved effective gastrointestinal delivery of nonsteroidal anti-inflammatory drugs (NSAIDs) and inhibited inflammation, but also reduced NSAID-induced gastrointestinal irritation and promoted GIT mucosal healing, which were validated in gastritis and colitis models. Importantly, the introduction of Mt had resulted in a more stable release rate. In addition, the drug release rate of M-ZIF-8 can be regulated by changes in pH (Figure 13(c)). M-ZIF-8 had made significant progress in gastrointestinal delivery with a simple structure and good biocompatibility, which provided the inspiration to use Mt to build an oral drug delivery system.

Li et al.[99] developed a biocompatible chitosan/Mt (CS/Mt) microsphere as a loading and sustained release carrier for tanshinone IIA (TA) hydrophobic drugs. The CCK-8 cell viability assay showed that the resulting CS/Mt and TA@CS/Mt microspheres had no apparent cytotoxicity when the dose was less than 80 μg/mL (Figure 14(a,b)). The introduction of Mt into the chitosan matrix can enhance the encapsulation rate of the drug and delay the migration of the drug. The sample with a mass ratio of chitosan to Mt of 10:2 had the highest encapsulation efficiency (48.18 ± 2.54%), and the continuous cumulative drug release in phosphate buffer solution (pH 7.4) was the slowest (Figure 14(c, d)). It was found that the release kinetics of TA were consistent with the Higuchi model, and its release mechanism was not diffusion. This work provided a drug delivery system based on Mt, which was successfully applied to the

https://doi.org/10.1021/acsomega.4c00674
ACS Omega 2024, 9, 17760−17783

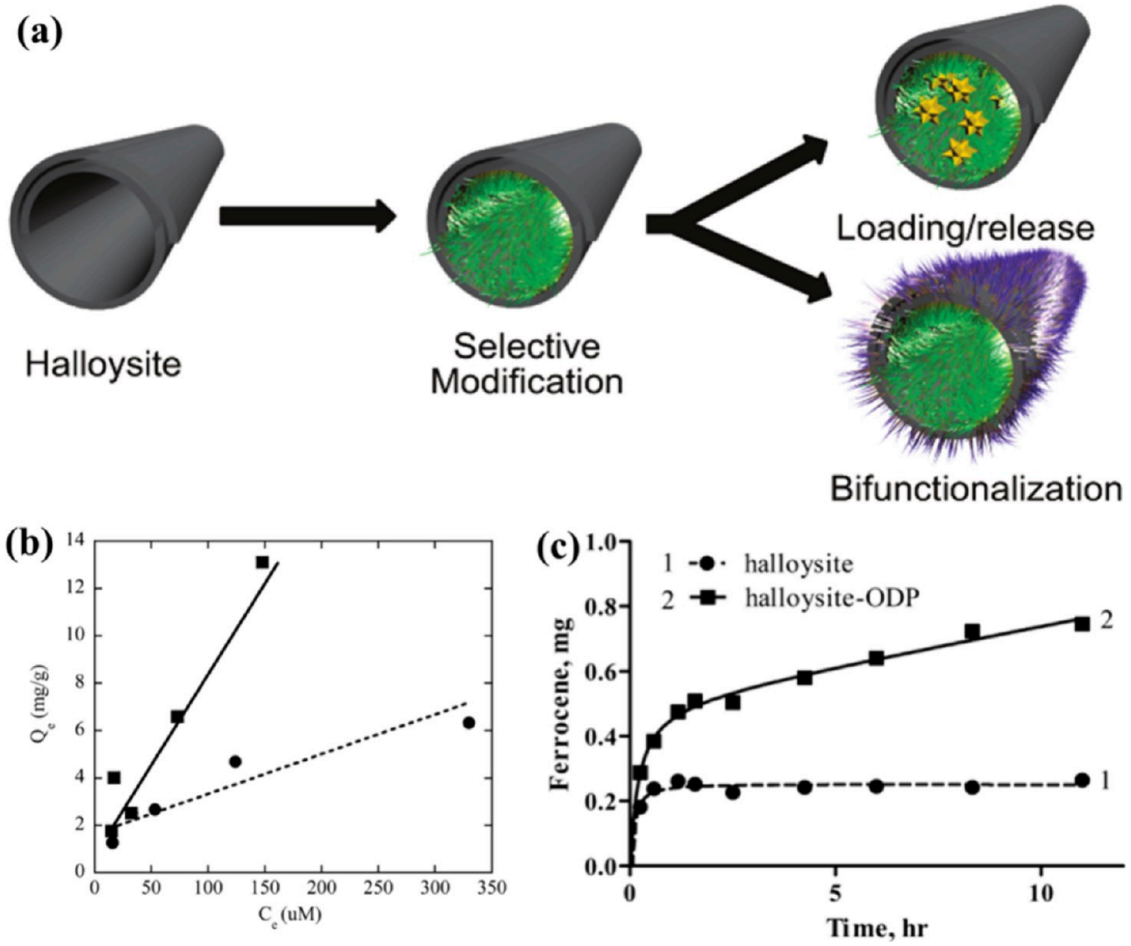

Figure 12. Drug release properties based on modified HNTs. (a) Schematic diagram of drug loading and release by HNTs. Equilibrium adsorption of ferrocene by HNTs (●) and HNTs-ODP (■) at room temperature from THF:H_2O (1:1) solution. (b) Release profile and (c) Higuchi square root of time plots for the release of ferrocene from HNTs (●) and HNTs-ODP (■). Reprinted with permission from ref 97. Copyright 2012 American Chemical Society.

preparation of a highly effective biocompatible drug delivery system for TA.

Betaolol hydrochloride (BH) has the ability to treat glaucoma, and its efficacy can be improved with reasonable dosage. Hou et al.[100] used the emulsifying solvent evaporation method to prepare propylene oxide nanoparticles loaded with BH intercalated with Mt for topical administration for the treatment of glaucoma (Figure 15(a)). The prepared Mt-BH nanoparticles have an average size and positive surface charge suitable for ophthalmic applications. The charge contributes to corneal adhesion and shows good stability to maintain the residence time on the corneal surface and ensure better drug release performance (Figure 15(b)). There was no significant bleeding except for the NaOH solution (positive group). However, according to the changes in the blood vessels, the order of irritation could also be as follows NaOH solution > BH solution > Mt-BH NPs > blank NPs > saline solution, indicating that although the irritancy of Mt-BH NPs was slightly higher than that of blank NPs due to the intrinsic irritancy of the active pharmaceutical ingredient (API) itself adsorbed on the surface of the nanoparticles during preparation, the Mt-BH NPs formulation was low in irritancy and well tolerated (Figure 15(c)). The formulation was suitable for clinical antiglaucoma use and was expected to be used in future pharmacokinetic studies in the future such as tear clearance. Feng et al.[101] used an improved solvent extraction/evaporation technique to prepare paclitaxel-loaded PLGA/Mt nanoparticles and modified them with trastuzumab. The drug exhibited a biphasic drug release profile with a moderate initial burst release followed by a sustained release profile. Experimental studies in vivo and in vitro showed that the drug had achieved significantly higher cellular uptake efficiency and targeting effects.

Kaol, which has similar properties to Mt, is also an ideal alternative material for drug delivery. Yang et al.[102] successfully prepared 2D Kaol-based drug delivery systems (DDSs) through the intercalation of organic guest species with different chain lengths. Kaol intercalation compounds exhibited high levels of biocompatibility and extremely low toxicity to most cancer cells. The prepared nanocomposites showed pH-sensitive release behavior and enhanced therapeutic effects on ten model cancer cell cultures, and are considered as promising candidates for new DDSs and tissue engineering applications. Cisplatin, cis-dichlorodiammineplatinum(II) (CDDP) is an anticancer drug with a side effect of bone marrow suppression. Toyota et al.[103] investigated the complex formation of allophane NPs with CDDP against A549 cells. The results showed that CDDP-allophane NPs were released under acidic and neutral pH conditions. The release was higher in acidic medium,

https://doi.org/10.1021/acsomega.4c00674
ACS Omega 2024, 9, 17760−17783

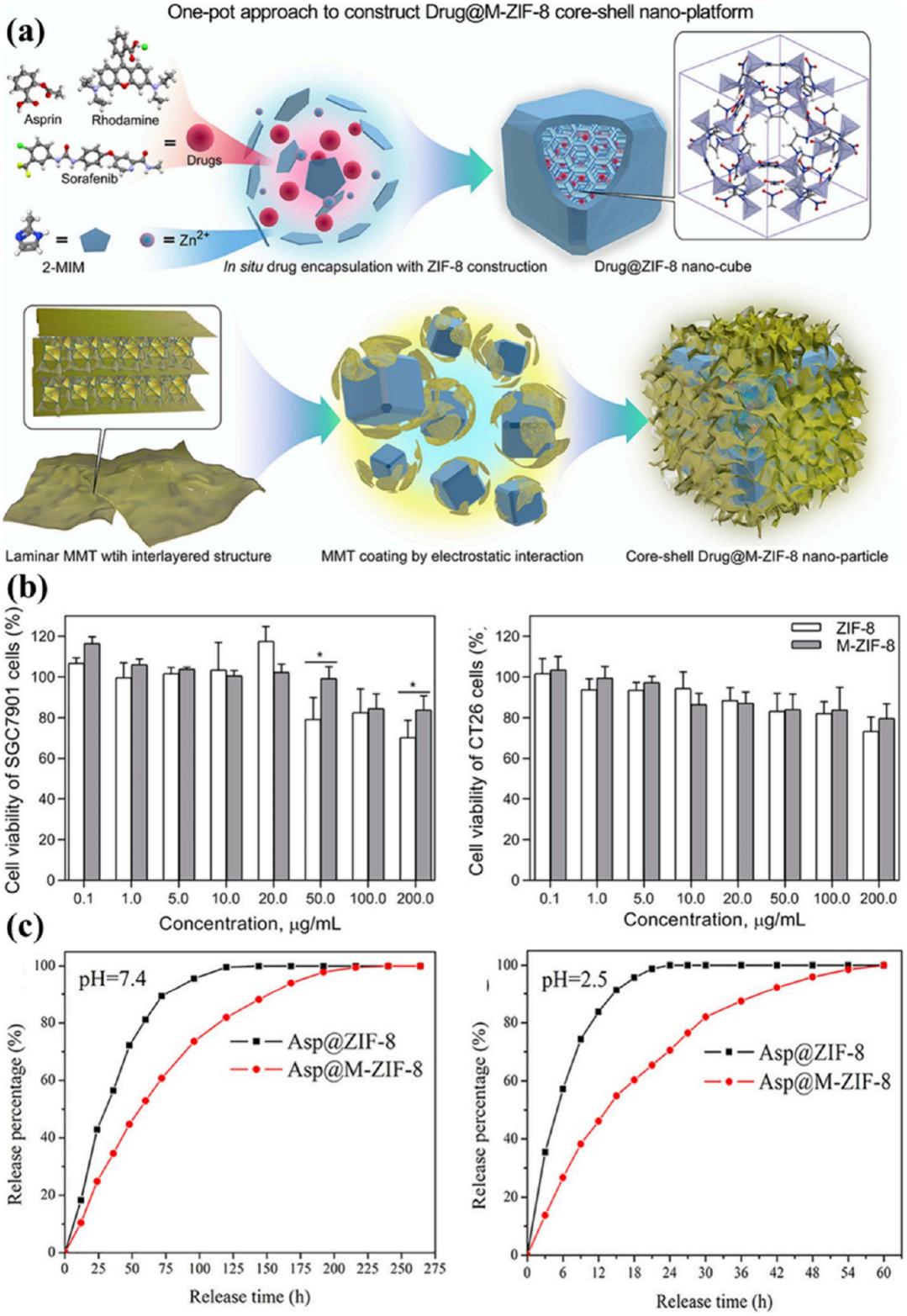

Figure 13. Asp release properties of M-ZIF-8. (a) Scheme of the one-pot preparation of the drug@M-ZIF-8 nanoplatform. (b) Cell viability of SGC7901 and CT26 cells treated with ZIF-8 and M-ZIF-8 for 24 h. Data are expressed as mean ± s.d. (n = 5). (c) The pH-responsive release profiles of Asp from Asp@ZIF-8 and Asp@M-ZIF-8 determined by UV−vis spectrophotometry. Reprinted with permission from ref 47. Copyright 2020 Elsevier.

where about 60% of CDDP was released in the first 50 h, whereas at pH 7.4, about 44% of CDDP was released within 70 h, showing a sustained release profile. Fluorescence microscopy showed that CDDP-allophane NPs were internalized by A549 cells. In addition, CDDP-allophane NPs were less cytotoxic than free CDDP at the same dose.

Structural and morphological advantages are the main reasons for their use as sustained release drug carriers. HNT

https://doi.org/10.1021/acsomega.4c00674
ACS Omega 2024, 9, 17760−17783

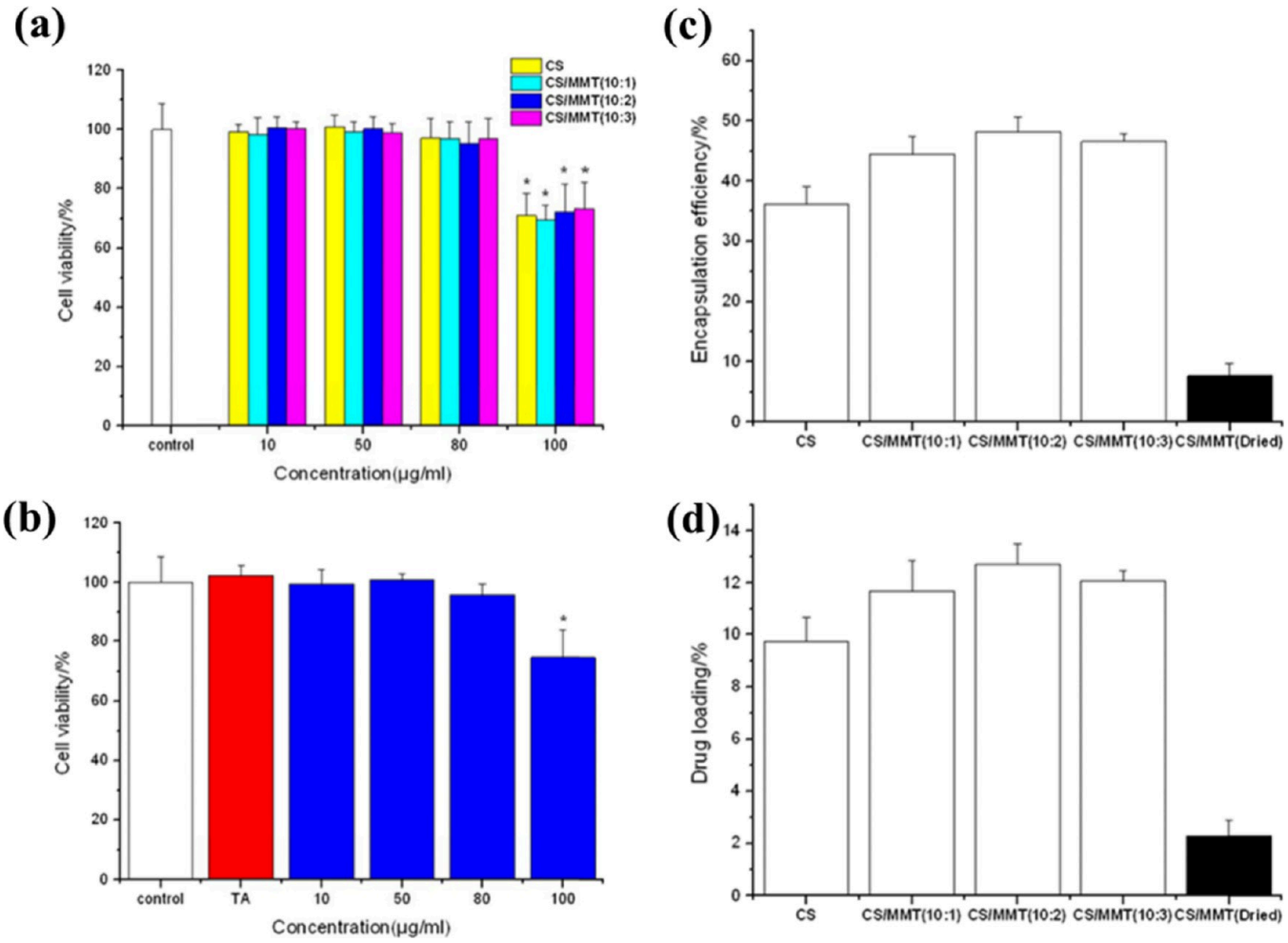

Figure 14. TA release properties of TA@CS/Mt. Cell viability (%) after contact with different kinds and concentrations of (a) CS/Mt microspheres and (b) different concentrations of TA@CS/Mt (10:2). Effect of Mt content on (c) encapsulation efficiency and (d) drug loading of CS/Mt microspheres. Reprinted with permission from ref 99. Copyright 2019 Elsevier.

with a hollow structure and Kaol and Mt with a layered structure are often used as important raw materials for drug loading. Sufficient structural space and easily modifiable surface functional groups (e.g., −OH) are used as storage sites for drugs such as CS and CPT. In addition, the binding of functional groups to the drug changes under different pH conditions, which is often important for use as a controlled release composite.

3.3. Detection. In vitro detection is characterized by large scale, rapid, and multiple reproducibility. Through the chemical reaction between the detection agent and the target, we can establish a concentration relationship to accurately know the amount of the target. In general, NNMs have a negative surface charge due to the residual electrons generated when a high valence atom is replaced by a low valence atom in the homogeneous process. Thus, the high specific surface area and the negative surface charge favor target binding. In addition, NNMs can also be used as carriers for detection agents thereby improving the efficiency of detection agent utilization.

The surface of APT is permanently negatively charged, which is conducive to the formation of cation exchange capacity to bind molecules with positive points on the surface. Wang et al.[48] had developed a novel nonenzymatic glucose electrochemical luminescence (ECL) sensor based on the integration of APT and semiconductor titanium dioxide (Figure 16(a)). Figure 16(b) shows the glucose concentration-dependent ECL intensity and the corresponding calibration curve (Figure 16(c)). As the glucose concentration increased, the ECL signal decreased accordingly, indicating that glucose can inhibit the ECL intensity of luminol in the presence of the catalyst APT-TiO_2 catalyst. In the range of 1.0 mM−1.0 nM, the inhibition rate has a linear relationship with the logarithm of the glucose concentration using a regression eq 3.

$$\text{Log I} = -0.17065\text{Log C} + 2.6874 \ (R = 0.9976) \quad (3)$$

And, the electrical activity interference from ascorbic acid (AA), dopamine (DA) and uric acid (UA) was negligible, indicating that the prepared biosensor had good selectivity for glucose (Figure 16(d)). In 14 consecutive measurements, the relative standard deviation (RSD) of the ECL response to 1.0 μM glucose was 0.7% (Figure 16(e)). Due to the stable structure of the APT-TiO_2, the reproducibility of this method was acceptable, giving an idea of APT as a sensor preparation material.[48]

2-D NNMs are currently being widely investigated for their ability to modulate ionic occupancy and thus improve the properties of composites. Wang et al.[104] prepared exfoliated kaol/manganese ferrite (E-Kaol/MFO) composites using a

https://doi.org/10.1021/acsomega.4c00674
ACS Omega 2024, 9, 17760−17783

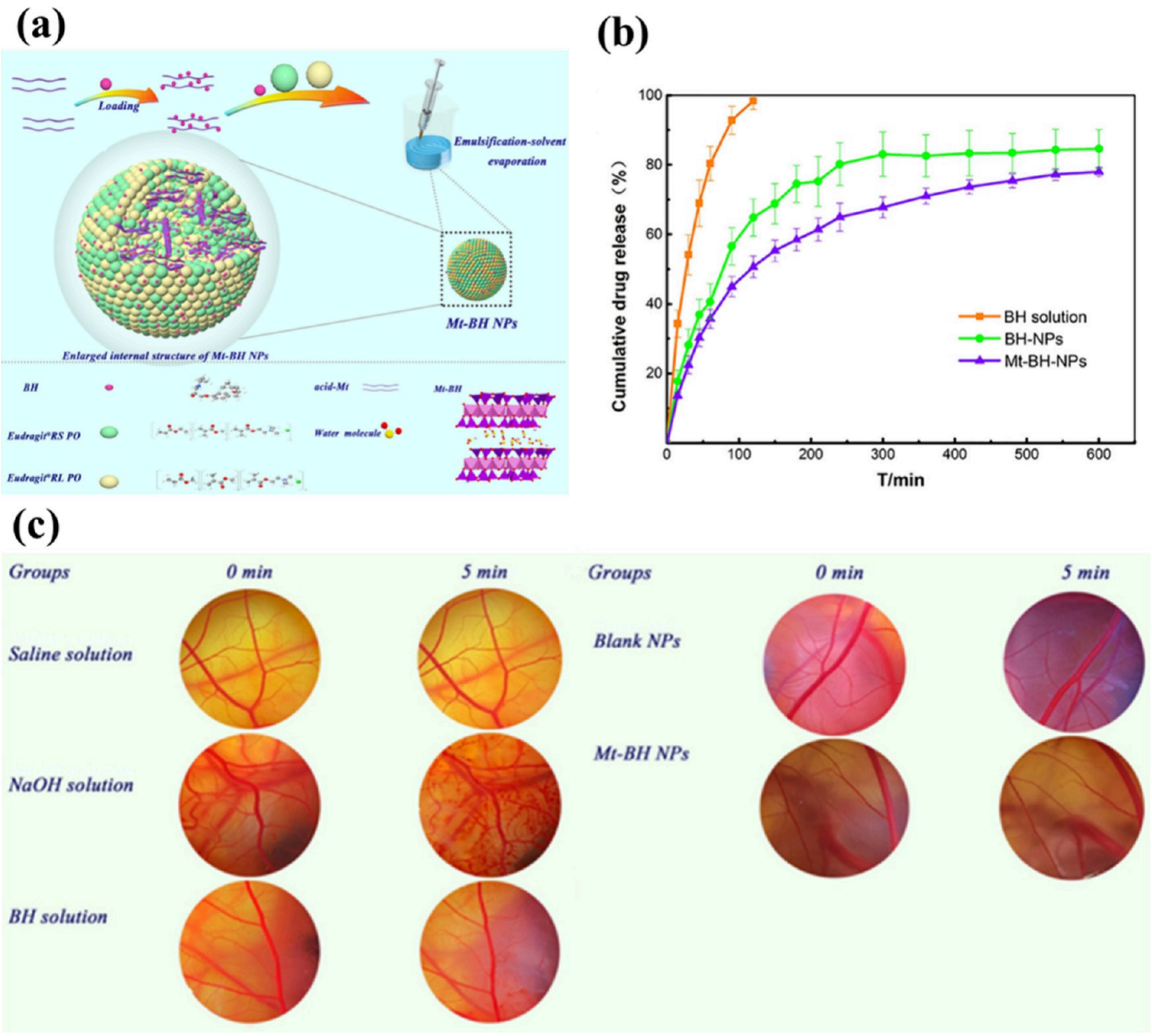

Figure 15. BH release properties of Mt-BH NPs (a) The illustration of the preparation procedure for Mt-BH NPs. (b) In vitro cumulative release curve of BH solution, BH NPs and Mt-BH NPs at the temperature of 34 ± 0.5 °C with oscillation frequency of 120 rpm. (c) The vascular congestion, hemolysis and coagulation of saline solution, NaOH solution, BH solution, blank NPs, Mt-BH NPs group. Reprinted with permission from ref 100. Copyright 2019 Elsevier.

one-step hydrothermal method to achieve highly sensitive detection of acid phosphatase (ACP) (Figure 17(a)). The exfoliated kaol facilitated the formation of defective MFO, enabling more iron cations to occupy the octahedral sites. This resulted in a significant increase in of various enzymatic activities. The colorimetric sensor prepared with E-Kaol/MFO demonstrated a wider detection range for ACP compared to MFO alone. It had a detection range of 0.5−3.0 mU/mL and a detection limit of 0.25 mU/mL. This work highlights the benefits of Kaol-modulated advanced enzyme mimics preparation and their potential for visual detection of disease markers. High-performance and biocompatible fingerprint powders are essential for clear and reliable latent fingerprints (LFP) imaging. Ni et al.[105] prepared berberine chloride (BBC) mixed with natural Mt mineral (BBC/Mt). The BBC/Mt powder exhibited bright solid luminescence due to the restriction of intramolecular motions (RIM) effect. And, BBC/Mt was successfully used as a fingerprint powder with three levels of detail (Figure 17(b)).

Mt can improve the morphology of the composite sensing material, thereby improving detection performance. Wahid et al.[106] successfully prepared a 3-D layered flower-like Mt-zinc oxide microhybrid sensor as a super electrochemical sensor for the detection of diltiazem hydrochloride (DZM. HCl). The obtained hybrid material with 2.0% Mt exhibited the most perfect flower-like morphology, the highest surface area (190.06 m^2/g) and the lowest resistivity. Meanwhile, the modified sensor obtained by cyclic voltammetry retained excellent the electrical conductivity and electrocatalytic activity. Under the best working conditions, the sensor successfully reached the detection limit of 0.177 and 0.21 $nmol{\cdot}L^{-1}$ DZM. HCl, and can successfully detect it in

https://doi.org/10.1021/acsomega.4c00674
ACS Omega 2024, 9, 17760−17783

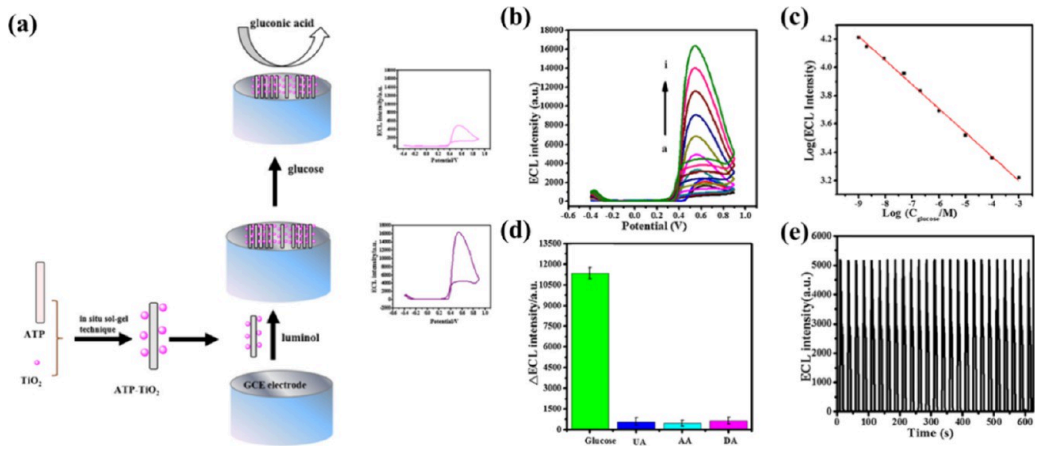

Figure 16. Detection properties of the APT-TiO_2-modified GCE. (a) The analytical procedure of the APT-TiO_2 electrode for glucose detection. (b) ECL responses of luminol on the APT-TiO_2-modified GCE to different concentrations of glucose. (c) Logarithmic calibration curve of the prepared glucose biosensor. (d) ECL signal specificity of the sensor toward 1.0 μM glucose, 30 nM AA, 30 nM DA and 30 nM UA on the APT-TiO_2-modified GCE in PBS (pH 7.4) containing 0.35 mM luminol. (e) The successive cyclic ECL responses of the biosensor to 1.0 μM glucose for 14 times. Reprinted with permission from ref 48. Copyright 2016 Elsevier.

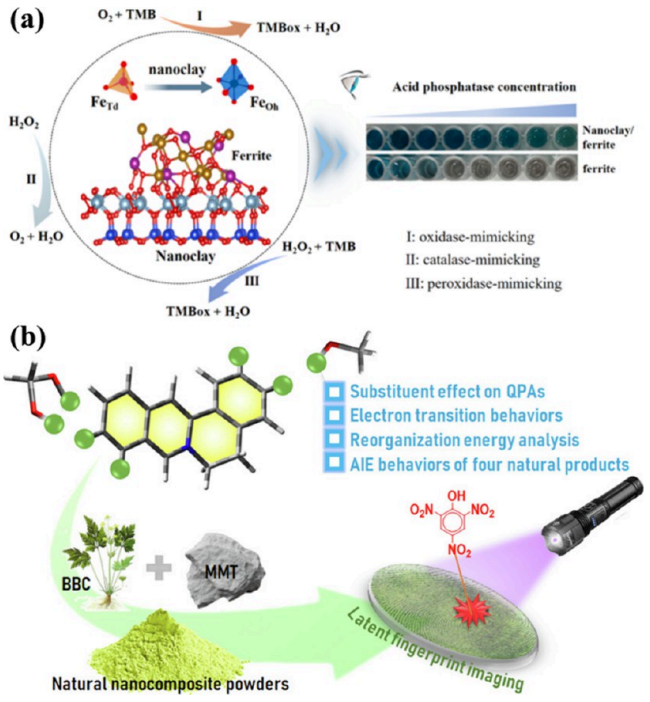

Figure 17. (a) Schematic representation of multienzymatic activities and ACP detection of E-Kaol/MFO. Reprinted with permission from ref 104. Copyright 2023 American Chemical Society. (b) Schematic representation of BBC/Mt for visualizing high-resolution LFP. Reprinted with permission from ref 105. Copyright 2023 Elsevier.

commercial and human biological fluids (serum samples). The constructed Mt-based sensor achieved reasonable accuracy and was not affected by other conventional pharmaceutical excipients.

3.4. Diagnosis. In addition to detection, NNMs are now being used in more advanced diagnostic area. In particular, in vivo diagnostics require good biocompatibility, leading researchers to consider NNMs with stable chemical compositions and structures.

Taking advantage of the high chemical stability, good adsorption and cell compatibility of APT, Ma et al.[49] prepared APT@Fe_3O_4@Ru (Figure 18(a)) as a dual contrast agent for optical and magnetic resonance imaging. They evaluated the in vitro effect of APT@Fe_3O_4@Ru as a dual contrast agent and studied its distribution in vivo using MRI in a rabbit model. The CCK-8 test showed that even high concentrations of APT@Fe_3O_4@Ru NC had low toxicity to LO2 and HepG2 cells (Figure 18(b)), indicating that it could be applied in vivo without obvious cell damage. Magnetic nanocomposites can accumulate at tumors through the EPR effect and can effectively penetrate into tumor tissues through blood vessels. Meanwhile, they can be effectively metabolized without leaving any residues in the body. APT@Fe_3O_4@Ru can be used as a T_2 shortening agent in magnetic resonance imaging (Figure 18(c, d)). The results showed that APT@Fe_3O_4@Ru can be used for tumor detection and diagnosis. However, the additional experiments and safety evaluations required for in vivo diagnosis make NNMs less widely used at present. There are also some studies that mimic the in vivo environment for diagnostic studies. Hamachi et al.[107] developed an Mt-supramolecular hydrogel hybrid for polyamine fluorescence spectroscopy sensing, which can detect polyamines in biological fluid simulants by fluorescence, and achieve rapid and naked-eye detection. The detection sensitivity was close to the range required for cancer diagnosis and clinical use.

In Asia, hepatocellular carcinoma (HCC) is the most commonly diagnosed subtype of liver cancer. Magnetic resonance imaging (MRI) is a common method for accurately diagnosing HCC. FePt@Mt nanocomposites with varying magnetic properties were synthesized by Chan et al. using the one-pot method.[108] Tuning the ratio of Mt can increase the saturation magnetization strength of the nanocomposites, which is beneficial for applications related to magnetic thermotherapy and MRI imaging. The FePt@Mt has multifunctional properties, as it can enhance magnetic resonance imaging (MRI) signals for observing hepatocellular carcinoma (HCC) and can also be used as an inducer for magnetic fluid hyperthermia (MFH). Kaol has also been investigated for the diagnosis of HCC using a similar technique. Chan et al.[109] also synthesized FePt@Kaol nanocomposites using a one-pot method. The magnetic

https://doi.org/10.1021/acsomega.4c00674
ACS Omega 2024, 9, 17760−17783

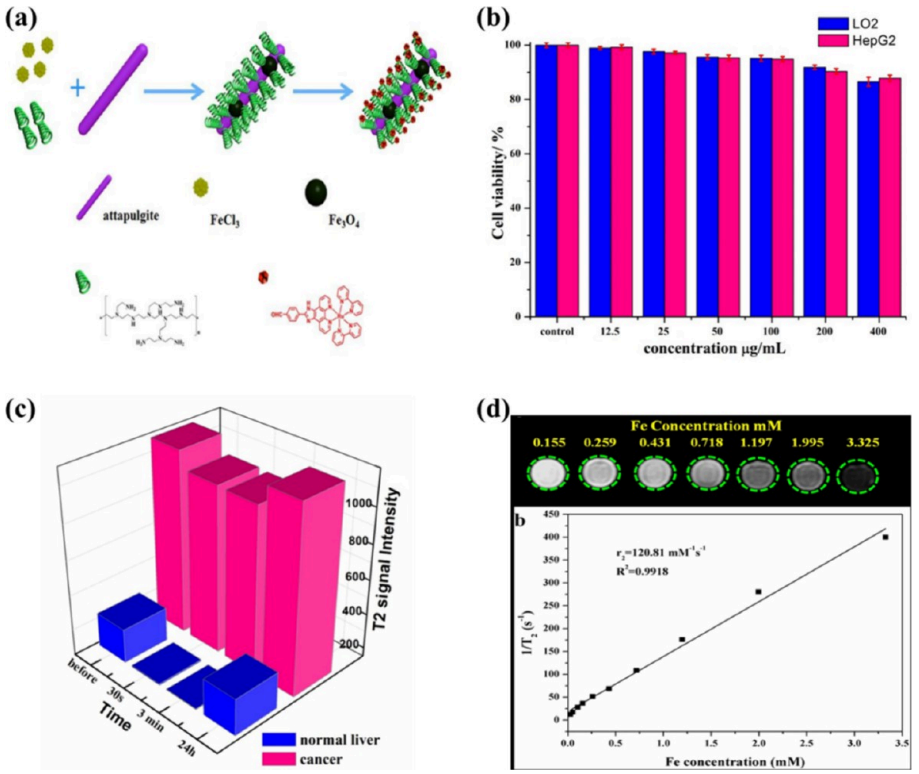

Figure 18. Imaging of APT@Fe_3O_4@Ru (a) Schematic representation of the preparation of APT@Fe_3O_4@Ru. (b) Viability of LO2 and HepG2 cells incubated with APT@Fe_3O_4@Ru at different concentrations for 24 h. (c) T2 signal intensity of normal liver and cancer at different times. (d) The linear fit of $1/T_2$ of the APT@Fe_3O_4@Ru with different Fe concentrations (0.026, 0.05, 0.104, 0.155, 0.259, 0.431, 0.718, 1.197, 1.995, 3.325 mM, respectively). Reprinted with permission from ref 49. Copyright 2017 Royal Society of Chemistry.

properties of the composite nanomaterials were found to depend on the proportion of kaol used. Increasing the proportion of kaol resulted in an increase in the saturation magnetization strength of FePt@Kaol. And, the nanocomposites achieved dual functionality, including MRI diagnostics and MRF therapy. In addition, the FePt@Kaol was recycled using the magnetic separation technique, achieving environmental friendliness. These two works demonstrate the positive role of 2-D NNMs in reducing the toxicity of composites and increasing the saturation magnetization strength of composite nanomaterials. It is shown that 2-D NNMs can be combined with magnetic materials and thus be used for diagnostic applications.

NNMs themselves have rarely been reported to function as diagnostics, which may be due to their stability and thus weaker function. And, the development of detection devices using NNMs takes advantage of their modulation of the morphology and ionic occupancy of the composites. In addition, their good biocompatibility is also the basis for the future development of composites for in vivo diagnostics. their excellent biocompatibility.

3.5. Hemostasis and Wound Healing. Loss of bleeding control after trauma is associated with a high risk of death. The use of natural hemostatic minerals to effectively control bleeding has been documented in traditional Chinese medicine. Today, we know that NNMs contain a variety of essential trace elements, including Zn, Ca, Mg, etc., which are beneficial to blood clotting and promote cell growth. In addition, their good adsorption properties are conducive to adsorbing blood and killing bacteria, which due to their large surface area and intrinsic antibacterial activity.

Sandri et al. investigated the safety and wound healing properties of different various nanoclay/spring water hydrogels. The results showed that APT did not significantly affect cell viability to a large extent (≥80% cell viability), and had a relatively high cell compatibility. By using APT in the formulation of the hydrogel, a better wound healing effect was achieved, which encouraging the use of APT as a wound healing ingredient for the treatment of chronic wounds.[110] Yang et al.[50] developed a novel Kaol composite (α-Fe_2O_3−Kaol) for hemostasis. α-Fe_2O_3−Kaol acid can stop bleeding within approximately 183 ± 16 s, and its hemostatic activity was higher than that of related compounds FeOOH-Kaol crude acid (298 ± 14 s), γ-Fe_2O_3−Kaol crude acid (212 ± 11 s) and Fe_3O_4−Kaol crude acid (218 ± 15 s), while having good biocompatibility (Figure 19(a,b)). Experimental results in mice showed that after 10 days of treatment with α-Fe_2O_3−Kaol acid, the wound was almost completely healed, while wound tissues treated or untreated with other iron oxide Kaol samples repaired slowly (Figure 19(c)). This rapid effect was attributed to the effective absorption of fluid in the blood, platelet activation, Kaol inducing the coagulation cascade, and α-Fe_2O_3 inducing erythrocyte aggregation (Figure 19(d)). The biocompatibility, hemostatic activity and low cost of α-Fe_2O_3−Kaol acid made it a safe and effective agent for preventing massive blood loss after trauma.

2D NNMs have the potential to improve the mechanical properties of hemostatic materials and provide a control/slow-release drug system. Zhang et al.[111] developed an Ag-Mt/agarose(AG) composite gel sponge (AMA) with rapid hemostatic properties, long-lasting antimicrobial activity and good biocompatibility by copolymerizing Ag-Mt with AG

https://doi.org/10.1021/acsomega.4c00674
ACS Omega 2024, 9, 17760−17783

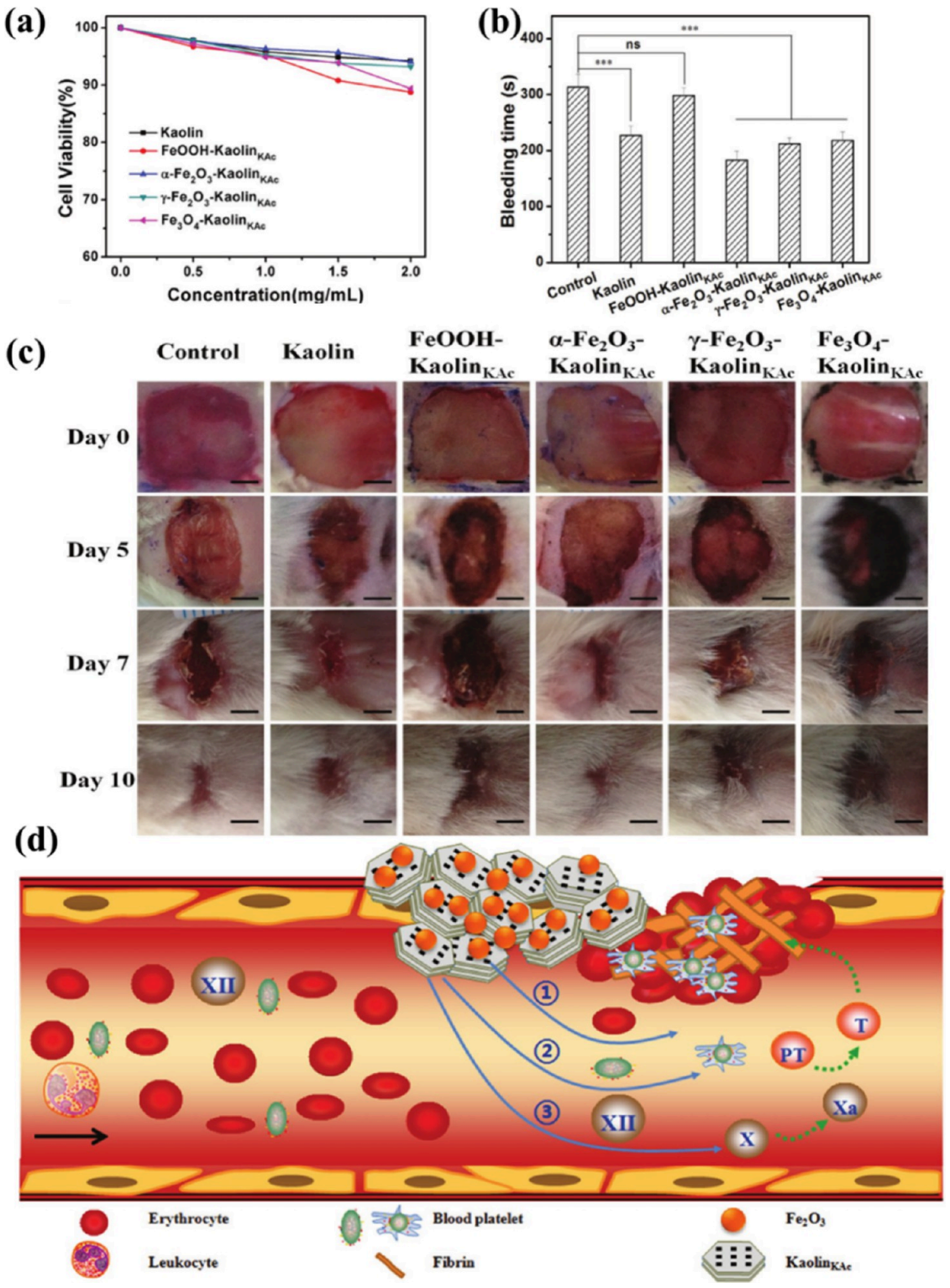

Figure 19. α-Fe_2O_3−Kaol for hemostasis. (a) Cytotoxicity of different concentrations of Kaol, FeOOH-Kaol, α-Fe_2O_3- Kaol, γ-Fe_2O_3−Kaol, and Fe_3O_4−Kaol incubated on L929 cells. (b) Bleeding time for wounds treated with samples or left untreated in the mouse tail vein incision model. (c) Digital images of wounds left untreated or treated with samples. (d) Illustration of the putative synergism of α-Fe_2O_3−Kaol in hemostasis. Reprinted with permission from ref 50. Copyright 2018 wiley.

hydrogel (Figure 20(a, b)). The introduction of Mt substantially improved the mechanical strength of AMA due to the formation of intermolecular hydrogen bonding between Mt and AG. As a result, AMA has good water absorption and retention capacity. Therefore, the hemostatic effect of AMA was significantly better than that of the AG gel sponge. In addition, the Ag^+ into the interlayer of Mt can stabilize it and slow down its release, resulting in a sustained drug release system (Figure 20(c)). This approach can achieve a long-lasting antimicrobial effect while significantly

https://doi.org/10.1021/acsomega.4c00674
ACS Omega 2024, 9, 17760−17783

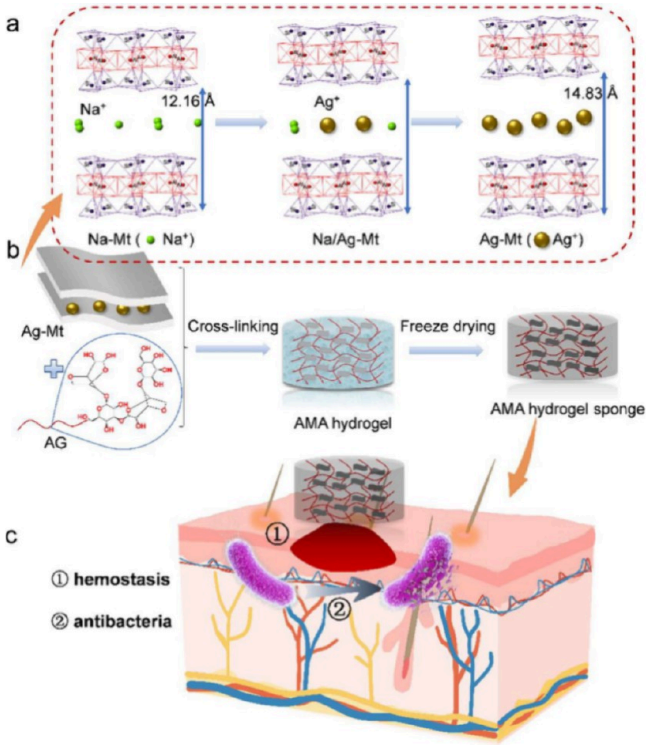

Figure 20. Schematic of (a) Ag-Mt and (b) Ag-Mt/AG gel sponge preparation. (c) Schematic diagram of Ag-Mt/AG gel sponge with effective hemostatic and antimicrobial ability for rapid wound healing. Reprinted with permission from ref 111. Copyright 2023 American Chemical Society.

improving the biocompatibility of AMA. Yang et al.[112] prepared an all-natural substance sponge (EMQS) composed of egg white (EW), quaternized chitin derivatives (QCs), and Mt. The addition of Mt improved the mechanical properties, resulting in a compressive strength of 0.126 MPa, and enhanced the hemostatic effect, with a hemostasis time of 49.7 ± 8.0 s. EMQS treatment enhanced the expression of growth factors, such as VEGF and TGF-β, resulting in accelerated dermal epithelial regeneration, enhanced angiogenesis and increased collagen deposition.

In addition, NNMs are also used for the adsorption of narcotics and drug overdoses due to their residual surface charge and large specific surface area. For example, Thiebault et al.[113] showed that Mt can be used as adsorbents for tramadol adsorption. Derivative data determined by a fitting procedure using the Langmuir, Freundlich and Dubinin−Radushkevich equation models clearly indicate that tramadol adsorption is primarily driven by electrostatic interactions with Mt. The studied tramadol was inserted into a monolayer arrangement in the interlayer space by cation exchange with Na+ cations in stoichiometric ratio, resulting in the amount of adsorbed tramadol matching the cation exchange capacity (CEC) of Mt. Besides, Karaman investigated the removal of a number of commonly used drugs from water using novel modified Mt and activated carbon. A wide range of drugs including: naproxen, diclofenac sodium, mefenamic acid, diazepam, and amoxicillin were effectively removed from water with good results in drug overdose and poisoning applications.

4. CHALLENGES AND PERSPECTIVES

Although NNMs have been widely used and have greatly contributed greatly to the development of the biomedicine, the further popularization and application still need to answer the following questions:

(1) Dispersibility. Currently, NNMs are easily agglomerated due to their large specific surface area and surface hydroxyl groups. Therefore, new methods, strategies and technologies are required for the pretreatment of NNMs, such as stirring and ultrasound or chemical treatment (such as acid or alkali treatment to remove impurity molecules on the surface) to improve their dispersion prior to application. In addition, NNMs can be effectively dispersed using spray-freeze-drying (SFD)techniques. For instance, Abdallah et al.[114] obtained well-dispersed Mt by SFD technique, which resulted in thinner silicate sheet layers of polypropylene nanocomposites.

(2) Homogeneity of the morphology and size. Due to their natural origin rather than artificial preparation, dimensional and size controllability are poor, which is unfavorable for their further development. It can be homogenized by a number of homogenizing operations to ensure as much homogeneity as possible. For example, 2-D NNMs can be stripped to ensure uniform dispersion and prevent size variations from stacking. Huang et al.[115] prepared obtained dispersions of Kaol through simple liquid-phase exfoliation, resulting composites exhibit high adsorption properties.

(3) Difficulty in functionalizing them through inorganic materials. Due to long-term deposition, the structure of NNMs is stable, which makes targeted modification by inorganic materials difficult. One effective solution to the difficulty of direct functionalization is to perform preliminary organic modification of the surface, followed by linking the corresponding functional groups.[116,117]

(4) The biological behavior of NNMs in vivo. The distribution, activity and metabolism of NNMs in vivo are unclear, which are key for the translational applications, including antibacterial, drug delivery, and theragnostic. Thus, a more systematic and comprehensive understanding of the bioeffects of NNMs is essential for medical translation. In order to solve this issue, our group is conducting a comprehensive evaluation of the biocompatibility and metal element dissolution of typical NNMs to advance their application in organisms.

As far as we know, the development direction of biomedicine should have the following characteristics:

(1) Biocompatibility, which cannot damage normal cells in the body.

(2) Targeting, which can directly enter the target pathological area.

(3) Nanosize, which can easily enter blood vessels, tissues and even cells smoothly in the body.

(4) Controlled or slow release, which can release drugs on demand using a “turn on/off” mechanism and release the drug slowly so that the drug can fully play its role in treating the disease.

(5) Low cost, which can benefit all people.

https://doi.org/10.1021/acsomega.4c00674
ACS Omega 2024, 9, 17760−17783

NNMs should be vigorously explored as potential biomedical materials with the above characteristics. Here, we propose the concept of natural nanomineral medical materials (NNMMs), which is intended to generate widespread research interest and commitment among scientists. They refer to NNMs that can be used in antimicrobial, diagnostic and therapeutic applications in vivo or in vitro, either on their own or as carriers, dispersants, enhancers, etc.

5. CONCLUSIONS

A systematic and pioneering summary of NNMs and their biological applications is important for their future development. In this review, we systematically introduce NNMs and classify them morphologically. Then, we introduce the medical application of some typical NNMs including APT, HNTs, and Mt in recent years, mainly focusing on antibacterial materials, detection, diagnosis, drug delivery. Furthermore, we have presented the challenges and perspectives of NNMs according to their current application. Finally, we propose a new concept of NNMMs to help people better understand this type of material and enable it to gain more biological applications. Due to their good biocompatibility, unique structure and excellent physicochemical properties, we believe that the application of NNMs in biomedicine will boom in the future. We hope that in the near future, NNMMs will become a new generation of biomedical hot materials like graphene to serve human life and health.

AUTHOR INFORMATION

Corresponding Authors

Yihe Zhang − *Engineering Research Center of Ministry of Education for Geological Carbon Storage and Low Carbon Utilization of Resources, Beijing Key Laboratory of Materials Utilization of Nonmetallic Minerals and Solid Wastes, National Laboratory of Mineral Materials, School of Materials Science and Technology, China University of Geosciences (Beijing), Beijing 100083, China*; orcid.org/0000-0002-1407-4129; Email: zyh@cugb.edu.cn

Peixia Wang − *National Anti-Drug Laboratory Beijing Regional Center, Beijing 100164, China; Beijing Narcotics Control Technology Center, Beijing 100164, China*; Email: sdwhwangpeixia@163.com

Authors

Feng Feng − *Engineering Research Center of Ministry of Education for Geological Carbon Storage and Low Carbon Utilization of Resources, Beijing Key Laboratory of Materials Utilization of Nonmetallic Minerals and Solid Wastes, National Laboratory of Mineral Materials, School of Materials Science and Technology, China University of Geosciences (Beijing), Beijing 100083, China*

Xiao Zhang − *Engineering Research Center of Ministry of Education for Geological Carbon Storage and Low Carbon Utilization of Resources, Beijing Key Laboratory of Materials Utilization of Nonmetallic Minerals and Solid Wastes, National Laboratory of Mineral Materials, School of Materials Science and Technology, China University of Geosciences (Beijing), Beijing 100083, China*

Bin Mu − *Key Laboratory of Clay Mineral Applied Research of Gansu Province, Lanzhou, Gansu 730000, China*

Wenjie Qu − *Engineering Research Center of Ministry of Education for Geological Carbon Storage and Low Carbon Utilization of Resources, Beijing Key Laboratory of Materials Utilization of Nonmetallic Minerals and Solid Wastes, National Laboratory of Mineral Materials, School of Materials Science and Technology, China University of Geosciences (Beijing), Beijing 100083, China*

Complete contact information is available at: https://pubs.acs.org/10.1021/acsomega.4c00674

Author Contributions

The manuscript was written by F.F. F.F., Y.Z., P.W., X.Z., B.M. and W.Q. revised and polished the paper. All authors discussed the results and commented on the manuscript.

Notes

The authors declare no competing financial interest.

ACKNOWLEDGMENTS

This work was supported by the National Natural Science Foundation of China (52072347), the Foundation of Key Laboratory of Clay Mineral Applied Research of Gansu Province, Lanzhou Institute of Chemical Physics, Chinese Academy of Sciences (CMAR-2022-04).

REFERENCES

(1) Zhang, G.; Liu, Y.; Zheng, S.; Hashisho, Z. Adsorption of volatile organic compounds onto natural porous minerals. *Journal of Hazardous Materials* **2018**, *364*, 317−324.

(2) Ha, W.; Wang, Z. H.; Zhao, X. B.; Shi, Y. P. Reinforced Supramolecular Hydrogels from Attapulgite and Cyclodextrin Pseudopolyrotaxane for Sustained Intra-Articular Drug Delivery. *Macromolecular Bioence* **2020**, *21*, e2000299.

(3) Liu, J.; Huang, Y.; Kumar, A.; Tan, A.; Jin, S.; Mozhi, A.; Liang, X. J. pH-sensitive nano-systems for drug delivery in cancer therapy. *Biotechnology Advances* **2014**, *32* (4), 693−710.

(4) Szczepanik, B. Photocatalytic degradation of organic contaminants over clay-TiO 2 nanocomposites: A review. *Applied Clay ence* **2017**, *141* (JUN.), 227−239.

(5) Lv, P.; Liu, C.; Rao, Z. Review on clay mineral-based form-stable phase change materials: Preparation, characterization and applications. *Renewable & Sustainable Energy Reviews* **2017**, *68* (part_P1)), 707−726.

(6) Mohammed, I.; Al Shehri, D.; Mahmoud, M.; Kamal, M. S.; Alade, O. S. A Surface Charge Approach to Investigating the Influence of Oil Contacting Clay Minerals on Wettability Alteration. *ACS OMEGA* **2021**, *6* (19), 12841−12852.

(7) Zhang, K.; Liu, Y.; Zhao, Z. R.; Shi, X. W.; Zhang, R. H.; He, Y. X.; Zhang, H. B.; Sun, Y.; Wang, W. J. Synthesis Technology of Magnesium-Doped Nanometer Hydroxyapatite: A Review. *ACS OMEGA* **2023**, *8* (47), 44458−44471.

(8) Wang, C.; Wang, S.; Kang, D. D.; Dong, Y. Biomaterials for in situ cell therapy. *BMEMat* **2023**, *1* (3), No. e12039.

(9) Liu, H.; Zhang, X.; Liu, J.; Qin, J. Vascularization of engineered organoids. *BMEMat* **2023**, *1* (3), No. e12031.

(10) Song, J.; Li, L.; Fang, L.; Zhang, E.; Zhang, Y.; Zhang, Z.; Vangari, P.; Huang, Y.; Tian, F.; Zhao, Y.; Chen, W.; Xue, J. Advanced strategies of scaffolds design for bone regeneration. *BMEMat* **2023**, *1* (4), No. e12046.

(11) Howes, P. D.; Chandrawati, R.; Stevens, M. M. Bionanotechnology. Colloidal nanoparticles as advanced biological sensors. *Science* **2014**, *346*, 1247390.

(12) Capadona, J. R.; Shanmuganathan, K.; Tyler, D. J.; Rowan, S. J.; Weder, C. Stimuli-Responsive Polymer Nanocomposites Inspired by the Sea Cucumber Dermis. *Science* **2008**, *319* (5868)), 1370−1374.

(13) Zheng, F.; Chen, Z.; Li, J. F.; Wu, R.; Zhang, B.; Nie, G. H.; Xie, Z. J.; Zhang, H. A Highly Sensitive CRISPR-Empowered Surface Plasmon Resonance Sensor for Diagnosis of Inherited

https://doi.org/10.1021/acsomega.4c00674
ACS Omega 2024, 9, 17760−17783

Diseases with Femtomolar-Level Real-Time Quantification. *Advanced Science* **2022**, *9* (14), 2105231.
(14) Wang, J.; Fu, Z.; Liu, H.; Zhao, W.; Zhu, B.; Dou, J.; Yu, H.; Chen, C. Preparation and characterization of micro-arc oxidation biological coatings on magnesium alloys containing graphene oxide. *Chemical Engineering Journal* **2024**, *482*, No. 149064.
(15) Wang, A. L.; Walden, M.; Ettlinger, R.; Kiessling, F.; Gassensmith, J. J.; Lammers, T.; Wuttke, S.; Peña, Q. Biomedical Metal-Organic Framework Materials: Perspectives and Challenges. *Advanced Functional Materials* **2023**, 2308589 DOI: 10.1002/adfm.202308589.
(16) Khan, K.; Tareen, A. K.; Iqbal, M.; Hussain, I.; Mahmood, A.; Khan, U.; Khan, M. F.; Zhang, H.; Xie, Z. Recent advances in MXenes: a future of nanotechnologies. *Journal of Materials Chemistry A* **2023**, *11* (37), 19764−19811.
(17) Su, L.; Qin, S.; Yu, X.; Chen, Y.; Wang, L.; Dong, W.; Xie, Z.; Zhang, H. NiCo LDH nanozymes with selective antibacterial activity against Gram-negative bacteria for wound healing. *J. Mater. Chem. B* **2023**, *11* (32), 7675−7683.
(18) Makvandi, P.; Wang, C. y.; Zare, E. N.; Borzacchiello, A.; Niu, L. n.; Tay, F. R. Metal-Based Nanomaterials in Biomedical Applications: Antimicrobial Activity and Cytotoxicity Aspects. *Adv. Funct. Mater.* **2020**, *30*, 1910021.
(19) Qi, G.-B.; Gao, Y.-J.; Wang, L.; Hao. Self-Assembled Peptide-Based Nanomaterials for Biomedical Imaging and Therapy. *Advanced materials* **2018**, *30*, 1703444.
(20) Tang, Z.; He, C.; Tian, H.; Ding, J.; Chen, X. Polymeric nanostructured materials for biomedical applications. *Prog. Polym. Sci.* **2016**, *60*, 86−128.
(21) Lin, Han; Chen, Yu; Shi, Jianlin Insights into 2D MXenes for Versatile Biomedical Applications: Current Advances and Challenges Ahead. *Advanced Science* **2017**, *5*, 1800518.
(22) Yang, Y.; Asiri, A. M.; Tang, Z.; Du, D.; Lin, Y. Graphene based materials for biomedical applications. *Mater. Today* **2013**, *16* (10), 365−373.
(23) Reshmy, R.; Philip, E.; Madhavan, A.; Sirohi, R.; Pugazhendhi, A.; Binod, P.; Awasthi, M. K.; Vivek, N.; Kumar, V.; Sindhu, R. Lignocellulose in future biorefineries: Strategies for cost-effective production of biomaterials and bioenergy. *Bioresource Technology* **2022**, *344*, 126241.
(24) Sun, L.; Bian, F.; Xu, D.; Luo, Y.; Wang, Y.; Zhao, Y. Tailoring biomaterials for biomimetic organs-on-chips. *Materials Horizons* **2023**, *10* (11), 4724−4745.
(25) Gammon, J. M.; Jewell, C. M. Engineering Immune Tolerance with Biomaterials. *Advanced Healthcare MATERIALS* **2019**, *8* (4), 1801419.
(26) Siswomihardjo, W. Biocompatibility Issues of Biomaterials. In *Biomaterials and Medical Devices: A Perspective from an Emerging Country*; Mahyudin, F.; Hermawan, H., Eds.; Springer International Publishing: Cham, 2016; pp 41−65.
(27) Smith, R. A.; Andrews, K. S.; Brooks, D. Cancer screening in the United States, 2018: A review of current American Cancer Society guidelines and current issues in cancer screening. *CA: A Cancer Journal for Clinicians* **2018**, *68* (4), 297−316.
(28) Caleyachetty, R.; Thomas, G. N.; Toulis, K. A.; Mohammed, N.; Gokhale, K. M.; Balachandran, K.; Nirantharakumar, K. Metabolically Healthy Obese and Incident Cardiovascular Disease Events Among 3.5Million Men and Women. *Journal of the American College of Cardiology* **2017**, *70* (12), 1429−1437.
(29) Amaia, C.-L.; Vetrano, D. L.; Graziano, O.; Gimeno-Feliu, L. A.; Carlos, C. S.; Angelo, C.; Pisciotta, M. S.; Sara, A.; F, M. R. J.; Giola, S. Assessing and Measuring Chronic Multimorbidity in the Older Population: A Proposal for Its Operationalization. *Journals of Gerontology* **2016**, *72* (10), 1417.
(30) Lounkine, E.; Keiser, M. J.; Whitebread, S. Large-scale prediction and testing of drug activity on side-effect targets. *Nature* **2012**, *486*, 361.
(31) Chen, H.; Li, J.; Li, T.; Xu, G.; Jin, X.; Wang, M.; Liu, T. Performance assessment of a novel medical-waste-to-energy design based on plasma gasification and integrated with a municipal solid waste incineration plant. *Energy* **2022**, *245*, No. 123156.
(32) Mei, X.; Hao, H.; Sun, Y.; Wang, X.; Zhou, Y. Optimization of medical waste recycling network considering disposal capacity bottlenecks under a novel coronavirus pneumonia outbreak. *Environmental Science and Pollution Research* **2022**, *29* (53), 79669−79687.
(33) Chen, Z.; Wu, C. S.; Yuan, Y. X.; Xie, Z. J.; Li, T. Z.; Huang, H.; Li, S.; Deng, J. F.; Lin, H. L.; Shi, Z.; Li, C. Z.; Hao, Y. B.; Tang, Y. X.; You, Y. H.; Al-Hartomy, O. A.; Wageh, S.; Al-Sehemi, A. G.; Lu, R. T.; Zhang, L.; Lin, X. C.; He, Y. Q.; Zhao, G. J.; Li, D. F.; Zhang, H. CRISPR-Cas13a-powered electrochemical biosensor for the detection of the L452R mutation in clinical samples of SARS-CoV-2 variants. *Journal of Nanobiotechnology* **2023**, *21* (1), 141.
(34) Chen, Z.; Li, J.; Li, T.; Fan, T.; Meng, C.; Li, C.; Kang, J.; Chai, L.; Hao, Y.; Tang, Y.; Al-Hartomy, O. A.; Wageh, S.; Al-Sehemi, A. G.; Luo, Z.; Yu, J.; Shao, Y.; Li, D.; Feng, S.; Liu, W. J.; He, Y.; Ma, X.; Xie, Z.; Zhang, H. A CRISPR/Cas12a-empowered surface plasmon resonance platform for rapid and specific diagnosis of the Omicron variant of SARS-CoV-2. *National Science Review* **2022**, *9* (8), nwac104.
(35) Valentino, C.; Rodríguez, T. M.; Benavides, P. H.; Vargas, F. A.; Paredes, J. M.; Rossi, S.; Sandri, G.; Medina Pérez, M. d. M.; Aguzzi, C. Human lactoferrin-clay mineral nanohybrids as emerging green biomaterials: A physicochemical characterization. *Appl. Clay Sci.* **2023**, *243*, No. 107085.
(36) Yang, Y.; Wang, X.; Yang, F.; Mu, B.; Wang, A. Progress and future prospects of hemostatic materials based on nanostructured clay minerals. *Biomaterials science* **2023**, *11* (23), 7469−7488.
(37) Gomes, C. D. F.; Silva, J. B. P. Minerals and clay minerals in medical geology. *APPLIED CLAY SCIENCE* **2007**, *36* (1−3), 4−21.
(38) Zou, Y. T.; Hu, Y. Z.; Shen, Z. W.; Yao, L.; Tang, D. Y.; Zhang, S.; Wang, S. Q.; Hu, B. W.; Zhao, G. X.; Wang, X. K. Application of aluminosilicate clay mineral-based composites in photocatalysis. *JOURNAL OF ENVIRONMENTAL SCIENCES* **2022**, *115*, 190−214.
(39) Grossman, M.; Bouville, F.; Erni, F.; Masania, K.; Libanori, R.; Studart, A. R. Mineral Nano-Interconnectivity Stiffens and Toughens Nacre-like Composite Materials. *Advanced materials* **2017**, *29* (8), 1605039.
(40) Zhou, C. H.; Keeling, J. Fundamental and applied research on clay minerals: From climate and environment to nanotechnology. *APPLIED CLAY SCIENCE* **2013**, *74*, 3−9.
(41) Brandão-Lima, L. C.; Silva, F. C.; Costa, P. V. C. G.; Alves-Júnior, E. A.; Viseras, C.; Osajima, J. A.; Bezerra, L. R.; de Moura, J. F. P.; de A. Silva, A. G.; Fonseca, M. G.; Silva-Filho, E. C. Clay Mineral Minerals as a Strategy for Biomolecule Incorporation: Amino Acids Approach. *Materials* **2022**, *15*, 64.
(42) Ping, Y.; Hu, X.; Yao, Q.; Hu, Q.; Amini, S.; Miserez, A.; Tang, G. Engineering bioinspired bacteria-adhesive clay nanoparticles with a membrane-disruptive property for the treatment of Helicobacter pylori infection. *Nanoscale* **2016**, *8* (36), 16486−16498.
(43) Tian, G.; Zhang, Y.; Jiang, Y.; Hu, P.; Wang, H.; Zhang, Y. Nanoscale zerovalent Iron-incorporated kaolinite for hemostatic and antibacterial applications. *Appl. Surf. Sci.* **2023**, *636*, No. 157879.
(44) Belkadi, A.; Meliani, M. F.; Mokhtar, A.; Djelad, A.; Abdelkrim, S.; Kebir-Medjhouda, Z. A.; Bengueddach, A.; Sassi, M. Amoxicillin loaded bentonite, advanced low-cost antibacterial and environmentally friendly materials. *J. Mol. Struct.* **2022**, *1270*, No. 133880.
(45) Kryuchkova, M.; Batasheva, S.; Akhatova, F.; Babaev, V.; Buzyurova, D.; Vikulina, A.; Volodkin, D.; Fakhrullin, R.; Rozhina, E. Pharmaceuticals Removal by Adsorption with Montmorillonite Nanoclay. *International Journal of Molecular Sciences* **2021**, *22*, 9670.
(46) Dong, W.; Lu, Y.; Wang, W.; Zhang, M.; Jing, Y.; Wang, A. A sustainable approach to fabricate new 1D and 2D nanomaterials

from natural abundant palygorskite clay for antibacterial and adsorption. *Chemical Engineering Journal* **2020**, *382*, No. 122984.
(47) Zhao, H.; Ye, H.; Zhou, J.; Tang, G.; Hou, Z.; Bai, H. Montmorillonite-Enveloped Zeolitic Imidazolate Framework as a Nourishing Oral Nano-Platform for Gastrointestinal Drug Delivery. *ACS Appl. Mater. Interfaces* **2020**, *12* (44), 49431−49441.
(48) Wang, Y.-Z.; Zhong, H.; Li, X.-R.; Liu, G.-Q.; Yang, K.; Ma, M.; Zhang, L.-L.; Yin, J.-Z.; Cheng, Z.-P.; Wang, J.-K. Nonenzymatic electrochemiluminescence glucose sensor based on quenching effect on luminol using attapulgite−TiO2. *Sens. Actuators, B* **2016**, *230*, 449−455.
(49) Zhu, T.; Ma, X.; Chen, R.; Ge, Z.; Xu, J.; Shen, X.; Jia, L.; Zhou, T.; Luo, Y.; Ma, T. Using fluorescently-labeled magnetic nanocomposites as a dual contrast agent for optical and magnetic resonance imaging. *Biomaterials science* **2017**, *5* (6), 1090−1100.
(50) Long, M.; Zhang, Y.; Huang, P.; Chang, S.; Hu, Y.; Yang, Q.; Mao, L.; Yang, H. Emerging Nanoclay Composite for Effective Hemostasis. *Adv. Funct. Mater.* **2018**, *28* (10), No. 1704452.
(51) Mousa, M. A. M.; Kim, Y.-H.; Evans, N. D.; Oreffo, R. O.; Dawson, J. Tracking cellular uptake, intracellular trafficking and fate of Laponite nanoparticles in human bone marrow stromal cells. *Nanoscale* **2023**, *15*, 18457.
(52) Li, S.; Mu, B.; Wang, X.; Wang, A. Recent researches on natural pigments stabilized by clay minerals: A review. *Dyes Pigm.* **2021**, *190*, No. 109322.
(53) Warr, L. N. Recommended abbreviations for the names of clay minerals and associated phases. *Clay Minerals* **2020**, *55* (3), 261−264.
(54) Majka, T. M.; Bartyzel, O.; Raftopoulos, K. N.; Pagacz, J.; Leszczynska, A.; Pielichowski, K. Recycling of polypropylene/montmorillonite nanocomposites by pyrolysis. *JOURNAL OF ANALYTICAL AND APPLIED PYROLYSIS* **2016**, *119*, 1−7.
(55) Chen, T.; Xie, Q.; Liu, H.; Xie, J.; Zhou, Y. Nano-Minerals and Nano-Mineral Resources. *Diqiu Kexue Zhongguo Dizhi Daxue Xuebao/earth Science Journal of China University of Geosciences* **2018**, *43* (5), 1439−1449.
(56) Liao, L. New Development of Functional Mineral Materials in China. *Kuei Suan Jen Hsueh Pao/ Journal of the Chinese Ceramic Society* **2011**, *39* (9), 1523−1530.
(57) Liu, X.; Zhang, F.; Jing, X.; Pan, M.; Liu, P.; Li, W.; Zhu, B.; Li, J.; Chen, H.; Wang, L. Complex silica composite nanomaterials templated with DNA origami. *Nature* **2018**, *559* (7715)), 593−598.
(58) Sarkar, P. K.; Chaudhary, A. K. Ayurvedic Bhasma: the most ancient application of nanomedicine. *Journal of entific & Industrial Research* **2010**, *69* (12), 901−905.
(59) Peixoto, D.; Pereira, I.; Pereira-Silva, M.; Veiga, F.; Hamblin, M. R.; Lvov, Y.; Liu, M. X.; Paiva-Santos, A. C. Emerging role of nanoclays in cancer research, diagnosis, and therapy. *Coordination Chemistry Reviews* **2021**, *440*, 213956.
(60) Toyota, Y.; Matsuura, Y.; Ito, M.; Domura, R.; Okamoto, M.; Arakawa, S.; Hirano, M.; Kohda, K. Cytotoxicity of natural allophane nanoparticles on human lung cancer A549 cells. *Appl. Clay Sci.* **2017**, *135*, 485−492.
(61) Wang, X.; Dai, L.; He, S.; Wang, Y.; Zhang, Y. A novel biomineralization regulation strategy to fabricate schwertmannite/graphene oxide composite for effective light-assisted oxidative degradation of sulfathiazole. *Sep. Purif. Technol.* **2023**, *312*, No. 123314.
(62) Zhan, J.; Li, Y.; Huang, M.; Zhao, L.; Zou, J.; Tian, D.; He, J.; Lei, Y.; Shen, F. Improvement of anaerobic digestion of food waste by addition of synthesized allophane. *Bioresour. Technol.* **2022**, *361*, No. 127653.
(63) Zhao, H.; Zhang, X.; Zhou, D. Collagen, polycaprolactone and attapulgite composite scaffolds for in vivo bone repair in rabbit models. *Biomedical materials* **2020**, *15* (4), 045022.
(64) Zhang, W.; Qian, L.; Ouyang, D.; Chen, Y.; Han, L.; Chen, M. Effective removal of Cr(VI) by attapulgite-supported nanoscale zero-valent iron from aqueous solution: Enhanced adsorption and crystallization. *Chemosphere* **2019**, *221*, 683−692.
(65) Cheng, C.; Gao, Y.; Song, W. Halloysite nanotube-based H2O2-responsive drug delivery system with a turn on effect on fluorescence for real-time monitoring. *Chemical Engineering Journal* **2020**, *380*, 122474.
(66) Lorenzo, L.; Giuseppe, C.; Stefana, M.; Giuseppe, L. Effects of halloysite content on the thermo-mechanical performances of composite bioplastics. *Applied Clay Science* **2020**, *185*, 105416.
(67) Lisuzzo, L.; Cavallaro, G.; Pasbakhsh, P.; Milioto, S.; Lazzara, G. Why does vacuum drive to the loading of halloysite nanotubes? The key role of water confinement. *Journal of Colloid and Interface ence* **2019**, *547*, 361.
(68) Zhao, H.; Zhang, X.; Zhou, D.; Weng, Y.; Qin, W.; Pan, F.; Lv, S.; Zhao, X. Collagen, polycaprolactone and attapulgite composite scaffolds for in vivo bone repair in rabbit models. *Biomedical materials* **2020**, *15* (4), No. 045022.
(69) Abdullayev, E.; Sakakibara, K.; Okamoto, K.; Wei, W.; Ariga, K.; Lvov, Y. Natural tubule clay template synthesis of silver nanorods for antibacterial composite coating. *ACS Appl. Mater. Interfaces* **2011**, *3* (10), 4040−6.
(70) Chen, X.-G.; Li, R.-C.; Zhang, A.-B.; Lyu, S.-S.; Liu, S.-T.; Yan, K.-K.; Duan, W.; Ye, Y. Preparation of hollow iron/halloysite nanocomposites with enhanced electromagnetic performances. *Royal Society Open Science* **2018**, *5* (1), No. 171657.
(71) Herrera, J. I.; Olmo, N.; Turnay, J.; Sicilia, A.; Lizarbe, M. A. Implantation of sepiolite-collagen complexes in surgically created rat calvaria defects. *Biomaterials* **1995**, *16* (8), 625.
(72) Sanchez, C.; Belleville, P.; Popall, M.; Nicole, L. Applications of advanced hybrid organic−inorganic nanomaterials: from laboratory to market. *Chem. Soc. Rev.* **2011**, *40* (2), 696−753.
(73) Li, Z.; Tang, R.; Liu, G. Immobilized into Montmorillonite Mn(II) Complexes of Novel Pyridine Schiff-Base Ligands and Their Catalytic Reactivity in Epoxidation of Cyclohexene with O2. *Catal. Lett.* **2013**, *143* (6), 592−599.
(74) Takahashi, C.; Shirai, T.; Hayashi, Y.; Fuji, M. Study of intercalation compounds using ionic liquids into montmorillonite and their thermal stability. *Solid State Ionics* **2013**, *241*, 53−61.
(75) Awad, M. E.; Lopez-Galindo, A.; Setti, M.; El-Rahmany, M. M.; Iborra, C. V. Kaolinite in pharmaceutics and biomedicine. *International journal of pharmaceutics* **2017**, *533* (1), 34−48.
(76) Long, M.; Zhang, B.; Peng, S.; Liao, J.; Zhang, Y.; Wang, J.; Wang, M.; Qin, B.; Huang, J.; Huang, J.; Chen, X.; Yang, H. Interactions between two-dimensional nanoclay and blood cells in hemostasis. *Materials science & engineering. C, Materials for biological applications* **2019**, *105*, No. 110081.
(77) Sun, Z.; Zhu, R.; Ding, T.; Zhang, X.; Li, C. Induced morphology orientation of α-FeOOH by kaolinite for enhancing peroxymonosulfate activation. *J. Colloid Interface Sci.* **2022**, *626*, 494−505.
(78) Saadh, M. J.; Abdulsahib, W. K.; Mustafa, A. N.; Zabibah, R. S.; Adhab, Z. H.; Rakhimov, N.; Alsaikhan, F. Recent advances in natural nanoclay for diagnosis and therapy of cancer: A review. *Colloids Surf., B* **2024**, *235*, No. 113768.
(79) Silva, D. T. C.; Arruda, I. E. S.; Araújo, J. I. R. d.; França, D. d. B.; Damasceno, B. P. G. d. L.; Oliveira, F. d. C. E. d.; Pessoa, C.; Soares, M. F. d. L. R.; Fonseca, M. G.; Soares-Sobrinho, J. L. Tamoxifen/montmorillonite as a controlled release oral system. *Journal of Drug Delivery Science and Technology* **2023**, *85*, No. 104572.
(80) Wang, H.; Sarwar, M. T.; Tian, L.; Bao, W.; Yang, H. Nanoclay Modulates Cation Occupancy in Manganese Ferrite for Catalytic Antibacterial Treatment. *Inorg. Chem.* **2022**, *61* (44), 17692−17702.
(81) Liu, J.; Zhang, Z.; Liu, Z.; Yu, Y. Preparation of a nanocomposite hydrogel with high adhesion, toughness, and inherent antibacterial properties by a one-pot method. *Colloids Surf., A* **2023**, *656*, No. 130368.
(82) Ismail, R. I. H.; Awad, H. A. S.; Shafik Emam, S.; Shady, N. M. A.; Fayez Ahmed, H.; Rabie, D. Evaluation of Smectite Effect as a Food Thickener in Gastroesophageal Reflux Disease in Neonates

https://doi.org/10.1021/acsomega.4c00674
ACS Omega 2024, 9, 17760−17783

Using Combined Esophageal Multichannel Intraluminal Impedance. *QJM: An International Journal of Medicine* **2023**, *116* (Supplement_1), hcad069.654.
(83) Qin, C.; Chen, C. Q.; Shang, C.; Xia, K. Fe3+-saturated montmorillonite effectively deactivates bacteria in wastewater. *SCIENCE OF THE TOTAL ENVIRONMENT* **2018**, *622*, 88−95.
(84) Yao, D. W.; Yu, Z. Z.; Li, N.; Hou, Y. N.; Xu, J. R.; Yang, D. J. Copper-modified palygorskite is effective in preventing and treating diarrhea caused by Salmonella typhimurium. *Journal of Zhejiang University. Science. B* **2017**, *18* (6), 474−480.
(85) Sajjad, W.; Khan, T.; Ul-Islam, M.; Khan, R.; Hussain, Z.; Khalid, A.; Wahid, F. Development of modified montmorillonite-bacterial cellulose nanocomposites as a novel substitute for burn skin and tissue regeneration. *Carbohydr. Polym.* **2019**, *206*, 548−556.
(86) Reddy, A. B.; Manjula, B.; Jayaramudu, T.; Sadiku, E. R.; Anand Babu, P.; Periyar Selvam, S. 5-Fluorouracil Loaded Chitosan-PVA/Na(+)MMT Nanocomposite Films for Drug Release and Antimicrobial Activity. *Nano-micro letters* **2016**, *8* (3), 260−269.
(87) Ge, M.; Li, J.; Song, S.; Meng, N.; Zhou, N. Development and antibacterial performance of silver nanoparticles-lecithin modified montmorillonite nanoparticle hybrid. *Appl. Clay Sci.* **2019**, *183*, No. 105334.
(88) de Souza, A. G.; dos Santos, N. M. A.; da Silva Torin, R. F.; dos Santos Rosa, D. Synergic antimicrobial properties of Carvacrol essential oil and montmorillonite in biodegradable starch films. *Int. J. Biol. Macromol.* **2020**, *164*, 1737−1747.
(89) Long, M.; Zhang, Y.; Shu, Z.; Tang, A.; Yang, H. Fe2O3 nanoparticles anchored on 2D kaolinite with enhanced antibacterial activity. *Chem. Commun.* **2017**, *53* (46), 6255.
(90) Ananyo, J. M.; Sourav, D.; Habeeb, R. A. P.; Bhaskar, D.; Jayabalan, R.; Susanta, K. B.; Mrutyunjay, S.; Tamhankar, A. J.; Amrita, M.; Cecilia, S. L. L. Doped ZnO nanoparticles impregnated on Kaolinite (Clay): A reusable nanocomposite for photocatalytic disinfection of multidrug resistant Enterobacter sp. under visible light. *J. Colloid Interface Sci.* **2018**, *530*, 610−623.
(91) Zhang, X.; Li, S.; Zhao, N.; Deng, Y.; Zuo, Z.; Li, C.; Zheng, S.; Sun, Z. Construction of organic compatible kaolinite antibacterial material via a dry process and its enhanced antibacterial activity. *Colloids Surf., A* **2023**, *657*, No. 130546.
(92) Zhu, T.; Ma, X.; Chen, R.; Ge, Z.; Xu, J.; Shen, X.; Jia, L.; Zhou, T.; Luo, Y.; Ma, T. Using fluorescently-labeled magnetic nanocomposites as a dual contrast agent for optical and magnetic resonance imaging. *Biomaterials Science* **2017**, *5*, 1090.
(93) Calderón-Larraaga, A.; Vetrano, D. L.; Ferrucci, L.; Mercer, S. W.; Marengoni, A.; Onder, G.; Eriksdotter, M.; Fratiglioni, L. Multimorbidity and functional impairment−bidirectional interplay, synergistic effects and common pathways. *Journal of Internal Medicine* **2019**, *285* (3), 255−271.
(94) Honary, S.; Zahir, F. Effect of Zeta Potential on the Properties of Nano-Drug Delivery Systems - A Review (Part 1). *Tropical Journal of Pharmaceutical Research* **2013**, *12* (2), 265−273.
(95) Svirskis, D.; Travas-Sejdic, J.; Rodgers, A.; Garg, S. Electrochemically controlled drug delivery based on intrinsically conducting polymers. *J. Controlled Release* **2010**, *146* (1), 6−15.
(96) Cheng, C.; Gao, Y.; Song, W.; Zhao, Q.; Zhang, H.; Zhang, H. Halloysite nanotube-based H2O2-responsive drug delivery system with a turn on effect on fluorescence for real-time monitoring. *Chemical Engineering Journal* **2020**, *380*, No. 122474.
(97) Yah, W. O.; Takahara, A.; Lvov, Y. M. Selective modification of halloysite lumen with octadecylphosphonic acid: new inorganic tubular micelle. *J. Am. Chem. Soc.* **2012**, *134* (3), 1853−9.
(98) Yahia, Y.; García-Villén, F.; Djelad, A.; Belaroui, L. S.; Sanchez-Espejo, R.; Sassi, M.; López-Galindo, A.; Viseras, C. Crosslinked palygorskite-chitosan beads as diclofenac carriers. *Appl. Clay Sci.* **2019**, *180*, No. 105169.
(99) Luo, C.; Yang, Q.; Lin, X.; Qi, C.; Li, G. Preparation and drug release property of tanshinone IIA loaded chitosan-montmorillonite microspheres. *Int. J. Biol. Macromol.* **2019**, *125*, 721−729.
(100) Zhao, Y.; Li, J.; Han, X.; Tao, Q.; Liu, S.; Jiang, G.; Zhu, G.; Yang, F.; Lv, Z.; Chen, Y.; Ping, Q.; Li, W.; Hou, D. Dual controlled release effect of montmorillonite loaded polymer nanoparticles for ophthalmic drug delivery. *Appl. Clay Sci.* **2019**, *180*, No. 105167.
(101) Sun, B.; Ranganathan, B.; Feng, S. S. Multifunctional poly(D,L-lactide-co-glycolide)/montmorillonite (PLGA/MMT) nanoparticles decorated by Trastuzumab for targeted chemotherapy of breast cancer. *Biomaterials* **2008**, *29* (4), 475−86.
(102) Zhang, Y.; Long, M.; Huang, P.; Yang, H.; Chang, S.; Hu, Y.; Tang, A.; Mao, L. Intercalated 2D nanoclay for emerging drug delivery in cancer therapy. *Nano Res.* **2017**, *10* (008), 2633−2643.
(103) Toyota, Y.; Okamoto, M.; Arakawa, S. New opportunities for drug delivery carrier of natural allophane nanoparticles on human lung cancer A549 cells. *Appl. Clay Sci.* **2017**, *143*, 422−429.
(104) Wang, H.; Bao, W.; Sarwar, M. T.; Tian, L.; Tang, A.; Yang, H. Mineral-Enhanced Manganese Ferrite with Multiple Enzyme-Mimicking Activities for Visual Detection of Disease Markers. *Inorg. Chem.* **2023**, *62* (21), 8418−8427.
(105) Ni, J.-S.; Lu, G.-H. Natural protoberberine alkaloid−montmorillonite nanocomposite powders with AIE features for visualizing high-resolution latent fingerprints. *Spectrochimica Acta Part A: Molecular and Biomolecular Spectroscopy* **2023**, *300*, No. 122908.
(106) Elfiky, M.; Salahuddin, N.; Matsuda, A. Green fabrication of 3D hierarchical blossom-like hybrid of peeled montmorillonite-ZnO for in-vitro electrochemical sensing of diltiazem hydrochloride drug. *Materials science & engineering. C, Materials for biological applications* **2020**, *111*, No. 110773.
(107) Yoshii, T.; Onogi, S.; Shigemitsu, H.; Hamachi, I. Chemically Reactive Supramolecular Hydrogel Coupled with a Signal Amplification System for Enhanced Analyte Sensitivity. *J. Am. Chem. Soc.* **2015**, *137* (9), 3360−3365.
(108) Chan, M.-H.; Lu, C.-N.; Chung, Y.-L.; Chang, Y.-C.; Li, C.-H.; Chen, C.-L.; Wei, D.-H.; Hsiao, M. Magnetically guided theranostics: montmorillonite-based iron/platinum nanoparticles for enhancing in situ MRI contrast and hepatocellular carcinoma treatment. *J. Nanobiotechnol.* **2021**, *19* (1), 308.
(109) Chan, M. H.; Hsieh, M. R.; Liu, R. S.; Wei, D. H.; Hsiao, M. Magnetically Guided Theranostics: Optimizing Magnetic Resonance Imaging with Sandwich-Like Kaolinite-Based Iron/Platinum Nanoparticles for Magnetic Fluid Hyperthermia and Chemotherapy. *CHEMISTRY OF MATERIALS* **2020**, *32* (2), 697−708.
(110) Garcia-Villen, F.; Faccendini, A.; Miele, D.; Ruggeri, M.; Sanchez-Espejo, R.; Borrego-Sanchez, A.; Cerezo, P.; Rossi, S.; Viseras, C.; Sandri, G. Wound Healing Activity of Nanoclay/Spring Water Hydrogels. *Pharmaceutics* **2020**, *12* (5), 467.
(111) Zhang, J.; Pan, Y.; Dong, S.; Yang, M.; Huang, Z.; Yan, C.; Gao, Y. Montmorillonite/Agarose Three-Dimensional Network Gel Sponge for Wound Healing with Hemostatic and Durable Antibacterial Properties. *ACS Applied Nano Materials* **2023**, *6* (18), 17263−17275.
(112) Yang, Y.; Zhang, H.; Zeng, F.; Jia, Q.; Zhang, L.; Yu, A.; Duan, B. A quaternized chitin derivatives, egg white protein and montmorillonite composite sponge with antibacterial and hemostatic effect for promoting wound healing. *Composites Part B: Engineering* **2022**, *234*, No. 109661.
(113) Thiebault, T.; Guégan, R.; Boussafir, M. Adsorption mechanisms of emerging micro-pollutants with a clay mineral: Case of tramadol and doxepine pharmaceutical products. *J. Colloid Interface Sci.* **2015**, *453*, 1−8.
(114) Abdallah, W.; Tan, V.; Kamal, M. R. The Effect of Spray-Freeze Drying of Montmorillonite on the Morphology, Dispersion, and Crystallization in Polypropylene Nanocomposites. *POLYMER ENGINEERING AND SCIENCE* **2020**, *60* (1), 168−179.
(115) Huang, X.; Tian, J.; Li, Y.; Yin, X.; Wu, W. Preparation of a Three-Dimensional Porous Graphene Oxide−Kaolinite−Poly(vinyl alcohol) Composite for Efficient Adsorption and Removal of Ciprofloxacin. *Langmuir* **2020**, *36* (37), 10895−10904.

https://doi.org/10.1021/acsomega.4c00674
ACS Omega 2024, 9, 17760−17783

(116) Lisuzzo, L.; Bertini, M.; Lazzara, G.; Ferlito, C.; Ferrante, F.; Duca, D. A computational and experimental investigation of the anchoring of organosilanes on the halloysite silicic surface. *Appl. Clay Sci.* **2023**, *245*, No. 107121.
(117) Tan, Y.; Xie, J.; Wang, Z.; Li, K.; He, Z. Effect of halloysite nanotubes (HNTs) and organic montmorillonite (OMMT) on the performance and mechanism of flame retardant-modified asphalt. *J. Nanopart. Res.* **2023**, *25* (4), 74.

https://doi.org/10.1021/acsomega.4c00674
ACS Omega 2024, 9, 17760−17783